British Geological Survey
NATURAL ENVIRONMENT RESEARCH COUNCIL

The micromorphology of the Quaternary deposits associated with the Carstairs Eskers, Lanarkshire, Scotland

Integrated Geological Survey (North)

Internal Report IR/02/097

BRITISH GEOLOGICAL SURVEY

INTERNAL REPORT IR/02/097

The micromorphology of the Quaternary deposits associated with the Carstairs Eskers, Lanarkshire, Scotland

Dr Emrys Phillips

Key words

Micromorphology, Carstairs, Quaternary deposits.

Bibliographical reference

PHILLIPS, E. R. 2002. The micromorphology of the Quaternary deposits associated with the Carstairs Eskers, Lanarkshire, Scotland. *British Geological Survey Research Report*, IR/02/097. 45pp.

Keyworth, Nottingham British Geological Survey 2002

BRITISH GEOLOGICAL SURVEY

The full range of Survey publications is available from the BGS Sales Desks at Nottingham and Edinburgh; see contact details below or shop online at www.thebgs.co.uk

The London Information Office maintains a reference collection of BGS publications including maps for consultation.

The Survey publishes an annual catalogue of its maps and other publications; this catalogue is available from any of the BGS Sales Desks.

The British Geological Survey carries out the geological survey of Great Britain and Northern Ireland (the latter as an agency service for the government of Northern Ireland), and of the surrounding continental shelf, as well as its basic research projects. It also undertakes programmes of British technical aid in geology in developing countries as arranged by the Department for International Development and other agencies.

The British Geological Survey is a component body of the Natural Environment Research Council.

Keyworth, Nottingham NG12 5GG

☎ 0115-936 3241 Fax 0115-936 3488
e-mail: sales@bgs.ac.uk
www.bgs.ac.uk
Shop online at: www.thebgs.co.uk

Murchison House, West Mains Road, Edinburgh EH9 3LA

☎ 0131-667 1000 Fax 0131-668 2683
e-mail: scotsales@bgs.ac.uk

London Information Office at the Natural History Museum (Earth Galleries), Exhibition Road, South Kensington, London SW7 2DE

☎ 020-7589 4090 Fax 020-7584 8270
☎ 020-7942 5344/45 email: bgslondon@bgs.ac.uk

Forde House, Park Five Business Centre, Harrier Way, Sowton, Exeter, Devon EX2 7HU

☎ 01392-445271 Fax 01392-445371

Geological Survey of Northern Ireland, 20 College Gardens, Belfast BT9 6BS

☎ 028-9066 6595 Fax 028-9066 2835

Maclean Building, Crowmarsh Gifford, Wallingford, Oxfordshire OX10 8BB

☎ 01491-838800 Fax 01491-692345

Parent Body

Natural Environment Research Council, Polaris House, North Star Avenue, Swindon, Wiltshire SN2 1EU

☎ 01793-411500 Fax 01793-411501
www.nerc.ac.uk

Foreword

This report is the published product of a study by the British Geological Survey (BGS) as part of their strategic regional geological mapping programme of the Midland Valley of Scotland. It describes the micromorphology of a suite of glacial sediments from the Carstairs area, Lanarkshire, Scotland. The work forms part of a multidisciplinary Midland Valley Project.

Contents

FIGURES

Figure 1. Annotated scanned image of the large format thin section taken from sample N2593 (see text for details). Scale bar = 10 mm.

Figure 2. Annotated scanned image of the large format thin section taken from sample N2594 (see text for details). Scale bar = 10 mm.

Figure 3. Annotated scanned image of the large format thin section taken from sample N2595 (see text for details). Scale bar = 10 mm.

Figure 4. Annotated scanned image of the large format thin section taken from sample N2596 (see text for details). Scale bar = 10 mm.

Figure 5. Annotated scanned image of the large format thin section taken from sample N2597 (see text for details). Scale bar = 10 mm.

PLATES

Plate 1. (a) General view of section exposed in Westend Wood sand and gravel quarry. The sand dominated sequence also contains a very coarse diamicton with 1 to 1.5 m diameter boulders of basalt. **(b)** Lower boundary separating the diamicton and the underlying sand dominated glaciofluvial sequence. Note that there is a distinctive clay and laminated silt-sand layer at the base of the diamicton, and that there is a lack of obvious disturbance within the underlying sediments. **(c)** Lower boundary of the mass flow deposit (diamicton) showing truncation of the clay layer and presence of a red coloured sandy horizon at the contact between the diamicton and underlying sediments.

Plate 2. (a) Bedded sand and gravel sequence in which the diamicton lacks the large boulders of basalt observed in the northern part of the section. **(b)** Close-up of boundary between the very coarse diamicton and the underlying sand dominated sediments. The boundary between the two units is marked by clay, overlain by laminated silt and sand, followed by red coloured sand. A sample tin has been inserted into the face across this complex sequence.

Plate 3. Photomicrographs of: **(a)** Hydrofracture filled by fine-grained, matrix-poor sand (scale bar = 2 mm); **(b)** Complex pattern of sand-filled hydrofractures with horizontal, bedding-parallel features occurring immediately below a prominent clay layer (see text for details) (scale bar = 2 mm); and **(c)** Small-scale folding and thrusting of a graded silt lamina (Scale bar = 2 mm). (sample N2593; plane polarised light).

Plate 4. Photomicrographs of: **(a)** Lenticular silty lamina containing fragments of coal cross-cutting laminated silt and clay (scale bar = 2 mm); **(b)** Poorly sorted sand with an open packed, ‘cement supported’ texture. Cement composed of a distinctive orange-brown clay (scale bar = 1 mm); and **(c)** Hydrofracture filled by fine-grained sand to coarse silt cross-cutting stratification in basal part of the diamicton (Scale bar = 2 mm). (a and b - sample N2593, c - sample N2594; plane polarised light).

Plate 5. Photomicrographs of: **(a)** Stratification within basal part of diamicton. Note cusp and flame structures developed along the boundary between the silt and clay layer and the adjacent diamicton, as well as the presence of circular and arcuate grain alignment structures within the matrix of the diamicton (scale bar = 2 mm); **(b)** Highly disrupted silt and clay layer within the diamicton characterised by the fragmentation of the more clay-rich laminae and partial liquefaction of the associated silt (scale bar = 2 mm); and **(c)** Wispy looking hydrofracture within a highly disrupted silt and clay layer filled by an orange-brown clay cutan (Scale bar = 2 mm). (sample N2594; plane polarised light).

Plate 6. Photomicrographs of: **(a)** Poorly sorted, matrix supported diamicton containing subrounded clasts of basalt, as well as more angular quartz and felsite (rhyolite) fragments (scale bar = 2 mm); **(b)** Poorly sorted diamicton containing a large, angular to subangular felsite (rhyolite) rock fragment. Also note there is a slightly more clay rich coating developed upon the lithic clast (scale bar = 2 mm); and **(c)** High-angle normal and reverse faults off-setting laminated clay and silt. Also note preferential fluidisation of the clay-poor, slightly coarser grained silt laminae (Scale bar = 2 mm). (a and b - sample N2594, c - sample N2595; plane polarised light).

Plate 7. Photomicrographs of: **(a)** Boundary between stratified diamicton and underlying matrix-poor sand. This boundary is deformed by a irregular silt-filled hydrofracture (scale bar = 2 mm); **(b)** Highly disrupted silty layer within the diamicton containing lithic fragments and till pebbles derived from the adjacent diamicton layers. Original clay laminae have been fragmented to form variably rounded mud clasts. Also note the presence of circular grain alignments within this silty layer (scale bar = 1 mm); **(c)** Highly disrupted silty layer within the diamicton containing lithic fragments and till pebbles derived from the adjacent diamicton layers. Original clay laminae have been fragmented to form variably rounded mud clasts (Scale bar = 2 mm); and **(d)** Finely laminated silt and clay layer at the base of the stratified diamicton. The layer is cut by an irregular hydrofracture filled by an orange-brown clay cutan (scale bar = 2 mm). (sample N2595; plane polarised light).

Plate 8. Photomicrographs of: **(a)** and **(b)** Moderately to poorly sorted, fine-grained sand with a variably developed clay cement. Also present are two elongate water escape conduits filled by an orange-brown, strongly birefringent clay cutan (scale bar = 2 mm). (sample N2596; a - plane polarised light, b - crossed polarised light).

Plate 9. Photomicrographs of: **(a)** Cusp and flame structure deforming boundary of a disrupted silt and clay layer within the stratified diamicton. Also note the presence of a circular arrangement of detrital grains (galaxy structure) within the diamicton which corresponds to the cusp formed at the boundary with the adjacent silt and clay layer (scale bar = 1 mm); **(b)** Lithic clast partially included within a disrupted silty layer (scale bar = 1 mm); **(c)** Cusp structure deforming boundary of a disrupted silt and clay layer within the stratified diamicton. Also note the presence of a circular arrangement of detrital grains (galaxy structure) within the diamicton which corresponds to the cusp formed at the boundary with the adjacent silt and clay layer (Scale bar = 1 mm); and **(d)** Highly disrupted silt and clay layer in which the silt laminae have undergone liquefaction (scale bar = 2 mm). (sample N2594; plane polarised light).

Plate 10. Photomicrographs of: **(a)** Folding within a disrupted silt and clay layer at the base of the stratified diamicton (scale bar = 2 mm); **(b)** Highly disrupted silt and clay layer containing stringers of diamicton. Also note that the silt laminae have undergone liquefaction (scale bar = 2

mm); **(c)** Highly disrupted silty layer containing lithic fragments and till pebbles derived from the adjacent diamicton layers. Original clay laminae have been fragmented to form variably rounded mud clasts. Also note presence of circular and arcuate arrangements of clasts within this disrupted silty layer (Scale bar = 2 mm); and **(d)** Highly disrupted silty layer containing lithic fragments, mud clasts and till pebbles derived from the adjacent diamicton layers. Also note presence of circular and arcuate arrangements of clasts within this disrupted silty layer (scale bar = 2 mm). (a and b sample N2594, c and d sample N2595; plane polarised light).

Plate 11. Photomicrographs of: **(a)** Highly disrupted silty layer containing lithic fragments, mud clasts and till pebbles derived from the adjacent diamicton layers. Also note presence of circular and arcuate arrangements of clasts within this disrupted silty layer (scale bar = 2 mm); **(b)** Highly disrupted silt and clay layer containing variably rounded mud clasts and till pebbles (scale bar = 2 mm); **(c)** Highly disrupted silty layer containing a large lithic fragments and variably rounded mud clasts. The lithic clasts is enclosed within a coating of fine-gained material similar to the matrix of the adjacent diamicton layers (Scale bar = 2 mm); and **(d)** Till pebble with distinct 'tail' (scale bar = 1 mm). sample N2595; plane polarised light).

Summary

This report describes the micromorphology of prepared samples of Quaternary sediments exposed in the Carstairs area of Central Scotland. The work forms part of the Midland Valley Terrane project of the Integrated Geological Survey (north) Programme.

The first part of the report provides the background information on the Quaternary geology of the Carstairs area. This is followed by a section describing the detailed micromorphology of five large format thin sections of the matrix of an unconsolidated very coarse diamicton and the underlying sands, silts and clay layers. The results are used to develop a model for the emplacement of a very coarse-grained mass flow deposit present within the Carstairs Quaternary sequence.

1 Introduction

This report describes the micromorphology of a sequence of glaciofluvial sediments associated with a major esker system developed in the Carstairs area, Lanarkshire, Scotland. The Quaternary geology of this area is dominated by a complex system of linear ridges, mounds and basins. The ridges have been interpreted as eskers which formed in an interlobate sediment sink which developed along the uncoupling margins of the Highland and Southern Uplands ice during Devensian deglaciation (Thomas and Montague, 1997). At this time the area between the margins of these uncoupling ice sheets was occupied by an extensive lake system which was fed by a major subglacial conduit which flowed towards the north-east.

Micromorphology is a relatively new and, currently, still developing technique and refers to the examination of Quaternary and other glacial sediments in thin section (see van der Meer, 1987, 1993; Menzies, 2000). A total of five large format thin sections of unconsolidated sediment from

Westend Wood sand and gravel quarry have been examined. The results are used to develop a model for the emplacement of a very coarse, laterally persistent mass-flow deposit which forms a distinctive unit within these glaciofluvial sediments.

2 Quaternary geology of the Carstairs area

The Quaternary geology of the Carstairs area is dominated by a complex system of linear ridges, mounds and basins. These geomorphological features have been variously interpreted as recessional moraines (Gregory, 1915; Charlesworth, 1926), kames, sub- or en-glacial eskers (Sissons, 1961; McLellan, 1969) or as landforms developed in response to supraglacial outwash fan sediments deposited on stagnant ice (Boulton, 1972; Bennett and Glasser, 1995).

More recently, Thomas and Montague (1997) have interpreted the ridges as eskers, formed in an interlobate sediment sink, developed between the uncoupling margins of the Highland and Southern Uplands ice during Devensian deglaciation. The area between these ice sheets was occupied by an extensive lake system which was fed by a major subglacial conduit which flowed towards the north-east. Thomas and Montague (1997) concluded that this conduit extended subaqueously to form a prominent single esker ridge across the lake floor.

On downwasting, the feeding conduit emerged at the surface of the ice to form a complex supraglacial outwash sandur. Sedimentological evidence presented by Thomas and Montague (1997) indicates that the surface of the sandur was cut by a number of large channels, filled by coarse gravel, which developed during periods of catastrophic flow. These channels also cut into the underlying ice and on abandonment and further downwasting were inverted to form a series of sub-parallel, weakly sinuous, apparently braided ridges. During a lower flow regime, extensive finer grained supraglacial sandur sedimentation took place on the periphery of these ridges, passing down-current across the ice margin into a series of fan-deltas extending into the expanding ice-front lake.

2.1 FIELD RELATIONSHIPS

The site which forms the main focus of this present study is located at the north-eastern end of the northern pit of Westend Wood sand and gravel quarry [NS 965 468]. This quarry is located in an area of subdued and irregularly distributed ridges, mounds, channels and basins equating to landform Assemblage B of Thomas and Montague (1997). The quarry area occurs on the immediate southern flank of the central section of the main esker ridge (Thomas and Montague, 1979, fig. 1). Boreholes and sediments exposed within the quarry show that the sequence in this area comprises a thick diamicton resting directly upon bedrock, which is in turn overlain by an approximately 30 m thick coarsening upwards succession of laminated silts, fine sands through fine to medium sand into sandy gravel and coarse gravel (Laxton and Nickless, 1980; Thomas and Montague, 1997). Detailed sedimentary logging carried out by Thomas and Montague (1997) indicates that the sequence fines towards the east, passing from thin diamictons (mass flow deposits), separated by parallel laminated sand and massive or cross-bedded pebble gravel, into parallel laminated sand and subordinate granule and pebble gravel and finally into thick successions of parallel-laminated sand, rippled fine sand and laminated and massive mud with occasional rhythmites (Thomas and Montague, 1997, fig 8). Palaeocurrent indicators, including

large-scale (c. 10 m in width) channel structures within the more proximal parts of the sequence, show that the main direction of flow was towards the south-south-east.

The site examined during this study occurs at the eastern end of the quarry within the more distal parts of this fluvioglacial sequence. The section (Plate 1) is mainly composed of a thick succession of well-bedded, parallel-laminated sands with occasional gravels (Plates 1 and 2), underlain by massive to weakly cross-laminated sands and silts with occasional layers of massive clay (Unit 1, Plate 1). These two sand dominated sequences are separated by a 2 to 3 m thick unit of very coarse diamicton (Plates 1b and c) containing large angular blocks (up to 1.5 m in diameter) of mainly locally derived Carboniferous basalt. This very coarse, laterally extensive diamicton was also recognised Thomas and Montague (1997). These authors reported blocks of felsite and 'quartz-porphyry' within the diamicton, which they believed to have been derived from the Devonian intrusions outcropping in the Tinto Hills approximately 10 km to the south-west. These boulders appear to occur in discrete pockets of lenses (see Plates 1 and 2) within the diamicton resulting in a rapid lateral variation in the thickness of this deposit. The matrix to the diamicton is composed of a highly deformed pebbly mud. The upper contact is partially obscured, but where exposed is apparently gradational into the overlying sands and gravels.

The base of the diamicton is sharp (erosive) with the larger clasts only locally protruding through into the underlying sediments (Plates 1 b and c). This lower boundary is immediately underlain by a 10 to 20 cm thick layer of massive to finely laminated red sand (Plates 1c and 2) which directly overlies and apparently cuts through a *c*. 10 cm thick layer of laminated silt and fine sand overlying a 3 to 10 cm thick band of massive, stiff clay (Plates 1c and 2b). At the central part of the section (Plates 1b and 1c) the laminated silt-sand and clay layers thin rapidly and are cut out by the erosive base of the diamicton. The sediments below this diamicton are essentially undeformed. However, a 10 to 15 cm thick layer of laminated silt, sand and silty sand within this underlying sequence (*c*. 30 cm below the base of the diamicton) is deformed by complex disharmonic to ptygmatic-looking folds indicative of soft sediment deformation.

Thomas and Montague (1997) interpreted this extremely coarse diamicton as a mass flow deposit. They argued that the angular nature of the clasts and highly restricted compositional range suggests that the diamicton was derived from a single point source. Furthermore, Thomas and Montague (1997) suggested that deposition of the diamicton possibly resulted from an extreme event in which ice-front supraglacial debris contained within a medial moraine, derived from an exposed nunatak (Tinto Hills), slumped catastrophically into the margin of the lake. However, for such a 'catastrophic event' (Thomas and Montague, 1979), the deposition of this diamicton had very little effect on the underlying sediments (see Plate 1b). The model proposed by Thomas and Montague (1997) for the deposition of this diamicton would require the southern margin of the lake to have abutted directly against the ice margin. In contrast, at the north-west margin of the lake, the ice-margin was fronted by a small fan-delta.

Examination (including thin sections) of the boulders within the diamicton suggest that they are mainly composed of locally derived Carboniferous basalt; including a distinctive ophimottled alkali basalt. Thin sections (S19319; S19639; S19642; S19643; S26395; S99844; S99845; S99846) of the Carboniferous basaltic lavas exposed in the Carstairs area reveal that some of these fine- to medium-grained basalts and trachybasalts are characterised by the presence of ophitic to sub-ophitic clinopyroxene within the groundmass defining a well-developed ophimottled texture. They are, in general, aphyric to porphyritic rocks which may possess a weakly to moderately well-developed pilotaxitic fabric. Phenocrysts, where present, are composed of anhedral to subhedral, twinned and zoned (simple and oscillatory) plagioclase. Plagioclase phenocrysts may define, or be aligned parallel to a pilotaxitic fabric present within the groundmass. The groundmass is fine- to medium-grained and comprises the assemblage plagioclase, clinopyroxene and opaque minerals with minor pseudomorphs (chlorite, serpentine) after possible olivine occurring in the more basic lithologies. Plagioclase forms variably aligned to randomly orientated laths. Pinky brown coloured, Ti-rich, clinopyroxene occurs intergranular

to plagioclase and forms rounded, anhedral to crudely elliptical (elongate) crystals. The elongate, elliptical crystals are locally shape aligned parallel to the pilotaxitic fabric. Pyroxene is variably altered to chlorite and/or carbonate, with irregular secondary carbonate locally mimetically replacing ophitic clinopyroxene in the most altered examples. An interstitial to intersertal, brown to grey coloured, glassy mesostasis is variably altered to chlorite, carbonate and opaque oxides. The ophimottled texture is a distinctive feature and has only been locally recorded within the Carboniferous Clyde Plateau Volcanic Formation exposed near: Calla Farm [NS 9952 4944] to the north of Carnwath; Yelping Craigs to south-east of Ampherlaw; near Bagmoors, Pettimain; and Greenaton [NS 9821 4814].

No Carboniferous lavas are exposed in the Tinto Hills, consequently it is unlikely that this area formed the original source of the detritus. However, Carboniferous basalt lavas (including ophimottled basalt) and rhyolitic/felsitic Devonian intrusive rocks are also exposed 4 to 5 km south of Carstairs in the area around Pettimain [NS 955 429] and Cairngryfe [NS 945 412], respectively. Similar basaltic igneous rocks dominate the solid geology in the immediate area of the Carstairs Eskers, underlying Rye Flat Moss [NS 953 482], Carnwath Moss [NS 975 479] and Harelaw [NS 916 477]; the latter located to the north-west of Carstairs. Based upon the petrological examination of thin sections within the BGS collection of Scottish rocks, it would appear that ophimottled alkali basalts are more widely developed in the area to the north of Carstairs. A relatively large Devonian rhyolitic intrusion occurs to the west of the Carstairs Eskers in the area of Blackhill [NS 830 440]. Consequently, the large angular boulders of basalt and rhyolite (felsite) within the diamicton may have been derived from the area immediately to the north or west of Carstairs, rather than the south as suggested by Thomas and Montague (1997).

3 Micromorphology

Five samples of unconsolidated sediment were collected along or immediately below the basal contact of one of the diamicton units exposed within Westend Wood sand and gravel quarry [NS 96665 46455]. The samples were collected using 10 cm square, aluminium kubiena tins which were either cut or pushed into the face of the exposure (Plate 2b). The samples were then removed and double sealed in plastic bags and stored at 4°C to prevent the material from drying out prior to sample preparation.

3.1 ANALYTICAL TECHNIQUES

A total of 5 large format thin sections were prepared by Mr D. Oates at the British Geological Survey's Thin Sectioning Laboratory (Keyworth) following the procedures for sample preparation of unconsolidated or poorly lithified materials. The thin sections were examined using a standard Zeiss petrological microscope and Zeiss projector enabling the analysis of both large and small-scale microscopic textures and fabrics. An annotated scanned image (Figures 1 to 5) of each thin section has been used to describe the main microscopic features developed within these Quaternary deposits.

3.2 TERMINOLOGY

The description and interpretation of the micromorphology and deformation structures developed within glacial deposits is a relatively recent and still developing technique (see van der Meer 1987, 1993; Seret 1993; van der Meer *et al*., 1990; van der Meer *et al*., 1992; van der Meer and Vegers, 1994; Menzies, 2000). Although repetitive features have been recognised by several workers (see van der Meer, 1987, 1993 and references therein), a standard nomenclature has yet to be formalised. The terminology used in this report is that proposed by van der Meer (1987, 1993) and Menzies (2000), and is based upon nomenclature developed by pedologists (for references see van der Meer, 1993). A definition of the terms used for the various textures and fabrics, and their proposed mode of formation is given below.

Plasmic fabric - The arrangement of high birefringent clay plasma/domains which are visible under the microscope (under cross polars) because of the similar extinction of similarly orientated domains. These fabrics are only observed when the sediment is clayey. Sediments which contain a limited amount of fines or relatively high proportion of carbonate within the matrix do not exhibit a well-developed plasmic fabric.

Unistrial plasmic fabric - A planar plasmic fabric defined by relatively continuous domains which is typically observed defining discrete shears. Interpreted as developing in response to planar movement (van der Meer, 1993).

Skelsepic plasmic fabric - A plasmic fabric in which the orientated domains occur parallel to the surface of large grains. Interpreted as developing in response to rotational movement (van der Meer, 1993).

Lattisepic plasmic fabric - A plasmic fabric defined by short orientated domains in two perpendicular directions. In many cases this fabric is found associated with a skelsepic plasmic fabric. Therefore, lattisepic plasmic fabrics are also interpreted as having developed in response to rotational movement (van der Meer, 1993).

Omnisepic plasmic fabric - A plasmic fabric in which all the domains have been reoriented. Interpreted as developing in response to rotational movement (van der Meer, 1993).

Till 'pebbles' - Formed by rotational movement (van der Meer, 1993). They are subdivided into three types: Type (1) consists of till which lack an internal plasmic fabric. They are defined by encircling voids and the shape of the 'pebbles' becomes progressively angular and flatter with depth; Type (2) is characterised by 'pebbles' of fine-grained material which were part of the original sediment host. They are recognised by an internal plasmic structure and are not defined by voids; Type (3) form isolated 'pebbles' of either till or fine-grained sediments and are usually interpreted as having formed by reworking of the till. They may or may not contain internal plasmic fabrics.

Other microscopic features - These include: the circular arrangement of clasts (skeleton grains) with or without a 'core stone', interpreted as having formed in response to rotation (van der Meer, 1993); pressure shadows which are also interpreted as having formed in response to rotation (van der Meer, 1993); dewatering structures associated with shearing; microboudinage; microscopic-scale primary sedimentary structures (e.g. lamination, cross-lamination….etc); water-escape structures associated with forceful dewatering; and crushing of clastic grains.

3.3 THIN SECTION DESCRIPTIONS

Collectors Number: EY413. **Registered Number:** N2593. **Location:** Westend Wood sand and gravel quarry. **Lithology:** laminated sand, silt and clay immediately below the base of the coarse diamicton.

Description: This thin section is of interlaminated sequence of fine-grained sand, coarse silt, fine silt and clay (Figure 1). For ease of description the sample has been divided into five units (A to E).

The lowest unit (Unit A) is at least 15 mm in thickness and is composed of massive, moderately sorted, coarse silt to very fine-grained sand which possesses a moderate to open packed texture with a moderate to high porosity. This sand to coarse silt contains only trace amounts of a finer grained clay matrix. Detrital grains are angular to subangular in shape with a low to moderate sphericity. They are mainly composed of monocrystalline quartz with subordinate to minor amounts of variably altered plagioclase and rock fragments. The composition of these lithic clasts is uncertain due to the very fine grain size of the sediment, but they appear to include mudstone and/or very fine igneous (possibly volcanic) rock fragments. Other minor to accessory detrital components include opaque minerals (including coal), white mica, bowlingite or chlorite aggregates and pseudomorphs after ferromagnesian minerals (i.e. olivine and/or pyroxene), amphibole and altered biotite.

The boundary of Unit A with the overlying layer is sharp, ranging from planar to slightly irregular in form and crossed by sand-filled hydrofractures (Figure 1). There is also a slight increase in the clay matrix component of Unit A sand towards this upper boundary.

The overlying Unit B is approximately 30 to 35 mm thick and composed of laminated fine to medium silt and silty clay (Plate 3a). Angular to subangular, low-sphericity detrital grains within the silt layers are mainly composed of monocrystalline quartz. However, flakes of white mica (probably muscovite) and granular to rod-shaped opaque grains are also common. The white mica flakes define a weak to very weakly developed fabric orientated at approximately 35° to bedding. As noted above, the lower boundary with the underlying sand is sharp with the upper boundary being gradational into the overlying more clay-rich unit (Unit C) (Figure 1). The base of Unit B is marked by a 0.3 to 0.9 mm thick lamina of clay to very fine clay-silt which contains angular, subangular to occasionally subrounded fragments of an opaque mineral and/or coal. This relatively clay-rich base is overlain by weakly normally graded silt which becomes more clayey towards the top of the unit. The primary sedimentary lamination in this part of the thin section is more diffuse in nature. Also present within this silt are two, low-angle silty-looking horizons that are darker in colour and inclined at approximately 20° to 25° to bedding. These features become wider downward and appear to link into the clay-rich layer present at the base of Unit B (Figure 1). There is no evidence of any deformation and/or displacement along these features which are cross-cut by the later sand-filled hydrofractures.

Unit B is cut by several subvertical fractures which are filled by very fine-grained sand (Plate 3a) which are interpreted to have been injected in a fluidised state from the underlying sand of Unit A. In the central to upper part of Unit B, these hydrofractures have led to the localised disruption of the sedimentary lamination. In the upper 5 to 6 mm of Unit B these near-vertical to steeply dipping structures are connected to a number of near-horizontal, bedding-parallel hydrofractures, which are also filled by very fine-grained, clean sand (Plate 3b). These fractures may locally exhibit a sigmoidal, en-echelon pattern (tension fissures) which yields a dextral sense of shear (south-easterly directed) in this plane of section. The more complex pattern of hydrofracturing, including bedding-parallel structures, within the upper part of Unit B may be related to the slight increase in clay content of the sediment and the presence of a 1.5 to 2.0 mm thick clay layer at the base of the overlying Unit C (Plate 3b; Section 4.4).

Unit C is composed of finely laminated clay and silty clay with a distinctive orange-red coloured (under plane polarised light), highly birefringent clay layer at the top of the unit (Figure 1). This

clay layer possesses a well-developed bedding-parallel plasmic fabric which is deformed by a set of micro-scale kinks. These kinks are developed at approximately 45° to 50° to bedding with the asymmetry of these structures yielding an apparent sinistral sense of shear in this plane of section. The plasmic fabric is also deformed adjacent to several water-escape structures which cross-cut Unit C. The formation of the plasmic fabric within the orange-red clay layer clearly pre-dates hydrofracturing and probably formed during the early stages of compaction (loading) and initial dewatering of this sedimentary sequence. Hydrofracturing of Unit C was apparently associated with the upward 'doming' or warping of this layer (Figure 1).

The upper boundary of Unit C is sharp, ranging from planar to slightly irregular in form (Figure 1); the latter possibly due to early sedimentary loading. This boundary is also locally disrupted by later hydrofracturing.

Unit D is composed of four distinct layers which form a weak concave to dish-shaped, open fold structure (Figure 1). The lowest layer is composed of reverse-graded fine to coarse silt, with the coarser grained, matrix-poor silt having apparently been injected into the upper parts of the layer fed by the hydrofractures in the underlying Unit C (see Figure 1). The reverse graded silt is overlain by a layer of laminated, very fine silt to silty clay. This layer varies in thickness, with soft sediment deformation resulting in localised folding and microfaulting (Plate 3c). In detail, these faults are diffuse structures and result in the marked attenuation of the lamination. This weakly deformed silty clay layer is overlain by reverse-graded, very fine to medium silt which is compositionally similar to the basal layer within Unit D.

At the top of Unit D is a compositionally distinct, lenticular, laterally impersistant layer composed of very fine silty clay containing angular, subangular and rounded coal fragments (Plate 4a). A weak circular arrangement of the finer grained clasts has been recorded developed around the larger coal fragments. This circular structure is accompanied by a very weakly developed skelsepic fabric which is partially defined by shape-aligned white mica flakes. Very fine hydrofractures within this coal-bearing layer are filled by a bright orange, strongly birefringent clay cutan. This clay fracture-fill is compositionally similar to the cement/matrix present within the overlying sand of Unit E and inferred to have been injected during hydrofracturing. The presence of a clay cutan within these hydrofractures also distinguishes these structures from the underlying sand filled fractures.

Unit E is composed of a laminated, fine- to medium-grained sand (Figure 1) with a distinctive open to very open packed, cement-supported texture (Plate 4b). The base of this sandy unit truncates the lamination in the underlying Unit D and cuts out the coal-bearing laminae at the top of this unit (Plate 4a). In detail, Unit E is composed of a layer of fine sand overlain by very fine sand or coarse silt. This fine sand to silt layer is in turn overlain by highly dilated, cement-supported medium-grained sand (Figure 1). The base of the upper sandy layer is sharp and erodes into the underlying finer grained unit. The sand at the base of Unit E possesses a weak reverse-grading with slightly coarser grained clasts (including coal/opaque fragments) occurring at the top of the layer.

The cement of all these sandy laminae is composed of an orange-brown, highly birefringent clay (Plate 4b) which, as noted above, is compositionally and morphologically similar to the clay cutan-filled hydrofractures. The plasmic fabric developed within the clay cement to the sand is unoriented or, locally, circular in form. This fabric is distorted around the clasts and is apparently a primary feature of the clay cement. In both the fine- and medium-grained sand laminae, very few of the clastic grains are in contact suggesting that cementation occurred when the sand was in a dilated (fluidised) state.

Detrital grains within the sandy laminae are angular to subangular in shape with a low to locally moderate sphericity. These clasts are mainly composed of monocrystalline quartz. Minor to accessory detrital components present within these sand layers include plagioclase, polycrystalline quartz, bowlingite/serpentine pseudomorphs after olivine and/or highly altered basalt, cryptocrystalline quartz, felsite, coal, opaque minerals, altered biotite, white

mica/muscovite, very fine-grained sandstone or siltstone rock fragments and rhyolitic rock fragments.

Collectors Number: EY414. **Registered Number:** N2594. **Location:** Westend Wood sand and gravel quarry. **Lithology:** boundary between laminated sand and overlying coarse diamicton.

Description: This thin section is of a unit of fine-grained sand to coarse silt overlain by stratified diamicton (Figure 2).

The lower part of the thin section is lithologically similar to Unit E of sample N2593. This sandy layer is approximately 35 mm thick and composed of weakly laminated fine sand to coarse silt. The lamination is defined by the variation in the modal proportion of an orange-brown cement and, to a lesser extent, grain size of the sediment (Figure 2). The boundaries between the laminae are slightly gradational or diffuse. The sandy laminae are in general poorly sorted, moderately to open packed with a variable clast- to cement-supported texture. The highly birefringent clay cement is morphologically similar to clay cutan and possesses a random, to weakly concentric plasmic fabric. This fabric is locally distorted between neighbouring detrital grains. In the sand laminae in which this cement is less well developed, the clay was noted lining or locally filling intergranular pore spaces. Formation of this clay cement clearly accompanied dilation of the sand, resulting in the development and preservation of the open packed, cement-supported texture.

Detrital grains are angular to subangular in shape with a low, to rarely, moderate sphericity. The clast assemblage within the sand laminae is dominated by monocrystalline quartz. Minor to accessory detrital components include plagioclase, opaque minerals, coal, mudstone, altered very fine-grained basalt, bowlingite/serpentinite pseudomorphs after a ferromagnesian mineral (olivine and/or pyroxene), chlorite, amphibole, apatite, muscovite, microcline and very fine-grained metasedimentary rock fragments. Some of the quartz grains possess relicts of an earlier-formed quartz overgrowth which probably partially formed the original cement in the source rock.

A slightly coarser grained sand layer at the top of this unit lacks the clay cement and has clearly been fluidised and injected into a hydrofracture which deforms the overlying diamicton (Plate 4c). The boundary between the sandy unit and the overlying diamicton is sharp, but may have been slightly modified during the fluidisation of the underlying sand.

The diamicton which forms the remainder of the thin section (Figure 2) possesses a streaky-looking, irregular stratification defined by elongate to lenticular bands or layers of silt and clay (Plate 5a). The clay and silt layers within the diamicton are lithologically similar to Unit D of sample N2593, and were probably derived from the underlying sedimentary sequence. These laminated silt and clay layers are inter-layered with a coarse, poorly sorted diamicton.

The original sedimentary lamination within the silt-clay layers is variably deformed and disrupted. This deformation resulted in the development of micro-scale disharmonic folds, flame structures as well as microfaults, fractures and/or shears (Plate 5a and b). Stretching (extension) of the clay-silt layers resulted in localised necking and microboudinage. In the most highly disrupted lenses the clay and silty clay laminae within these layers are fragmented or brecciated. The clay laminae sometimes possess a weakly to moderately developed plasmic fabric. In the least internally disrupted clay-silt layers, this plasmic fabric occurs parallel to the sedimentary lamination. However, in the more highly disrupted layers this fabric is deformed, indicating that foliation development occurred prior to the incorporation of the clay-silt into the diamicton.

In contrast to the clay, the interlaminated silts have undergone varying degrees of fluidisation (Plate 5b and c). Consequently, the more silty layers are internally more highly disrupted, comprising angular to subrounded fragments of finely laminated clay within a variably

homogenised silt matrix. These more highly disrupted clay-silt layers may be cut by, or contain fragments of clay-filled wispy-looking hydrofractures (Plate 5c).

The boundaries of the silt and clay layers with the adjacent diamicton are sharp, but vary from locally planar, irregular, flame-like to cuspate in form. Circular or spiral (galaxy, van der Meer, 1993) arrangements of clastic grains are locally present in the diamicton within the cusps, with the associated clay flames extending either side of these microstructures. Irregular fragments and elongate ribbons or silty and clay-rich material are present within the matrix of the diamicton layers. Rounded, irregular to tear drop-shaped fragments or 'clasts' of the matrix of the diamicton have also been noted within the more highly disrupted silt-clay layers. These 'clasts' are morphologically similar to the Type 1 till pebbles of van der Meer (1993) (see Section 4. 3).

In thin section it is evident that the diamicton layers are poorly sorted with a very open packed, matrix-supported texture (Plate 6a). The matrix is composed of a red-brown (under plain polarised light) clay-rich material, with the red colouration possibly due to a hematitic stain. The presence of this straining largely masks any plasmic fabric that may be present. However, a crude lattisepic plasmic fabric can locally be recognised. This fabric appears to have nucleated upon the margins of the included detrital grains. Clasts range from ≤ 0.1 mm to > 10 mm in diameter. These clasts are angular to subangular in shape with a low to moderate sphericity. The coarser grained clasts are locally enclosed within a coating or rim of slightly more clay-rich material (Plate 6b) which, in some cases, possesses a weakly developed skelsepic plasmic fabric. Circular and curved aggregates or arrangements of finer grained clasts, with or without a core stone, are relatively common within the diamicton layers (see Section 4.2). The bulk of the diamicton is, however, massive with very little evidence of solid-state deformation. The diamicton also contains irregular to wispy-looking clay cutan lined or filled fractures which are interpreted as defining fluid pathways which were active during the dewatering.

The larger detrital grains within the diamicton (Plate 6a and b) are mainly composed of altered basaltic rock fragments, pilotaxitic basalt, fine-grained quartzose litharenite, felsite, hematised siltstone or very fine-grained sandstone, polycrystalline quartz, hematised mudstone, hornblende-microporphyritic andesite, rhyolite, plagioclase-porphyritic andesitic rock and siltstone or very fine-grained wacke sandstone. The finer-grained, sand-grade detrital grains present within the diamicton layers are mainly composed of monocrystalline quartz. Minor to accessory detrital components present include polycrystalline quartz, opaque minerals, pseudomorphs after a ferromagnesian mineral (olivine and/or pyroxene), plagioclase amphibole and a very fine-grained schistose metasedimentary rock.

The presence of pinky-brown Ti-augite within basaltic rock fragments (Plate 6a) indicates that they are alkaline in character and, therefore, probably derived from the Carboniferous Clyde Plateau Volcanic Formation. In contrast, the more andesitic and rhyolitic (including felsite) rocks (Plate 6b) are believed to have been derived from the Biggar Volcanic Formation (or related Siluro-Devonian volcanic rocks) and Siluro-Devonian high-level intrusive rocks exposed in the Lanark district. The sedimentary rocks of the Siluro-Devonian Lanark Group, in particular the Swanshaw Sandstone Formation, probably provided the main source of the quartzose litharenite rock fragments present within the diamicton. The angular nature of the clasts within the diamicton supports the local derivation of this detritus. Furthermore, the preservation of bowlingite and/or serpentine pseudomorphs after olivine and pyroxene within the diamicton also indicates a local source for at least some of the detritus. These pseudomorphs are relatively weak and would have been destroyed during a prolonged period of transportation.

The lower part of the diamicton is cut by a hydrofracture filled by matrix-poor sand which is compositionally the same as, and was derived from the underlying laminated sand unit. Hydrofracturing of the diamicton and the accompanying fluidisation of the sand clearly post-dated deposition.

Collectors Number: EY415. **Registered Number:** N2595. **Location:** Westend Wood sand and gravel quarry. **Lithology:** boundary between laminated sand and overlying coarse diamicton.

Description: For ease of description this thin section is divided into three units (Figure 3). The lowest, Unit A, is composed of laminated silt and silty clay which is compositionally similar to Unit E of sample N2593. The lamination is deformed by at least one set of normal and reverse faults, with associated minor drag folding. The planes of these microfaults are rather diffuse due to the local injection of fluidised silt along these structures (Plate 6c). Liquefaction of the silt laminae has also resulted in the disruption of the original sedimentary lamination. The lamination within this unit defines a broad (centimetre scale), open synform (Figure 3).

The synform and microfaults developed within Unit A are truncated at the sharp base of the overlying unit (Unit B), the latter being composed of laminated silt, coarse silt and very fine sand (Figure 3). This micro-textural relationship clearly indicates that deformation (microfaulting) and liquefaction of the silty laminae of Unit A occurred prior to the deposition of Unit B. In detail, this silt and sand unit possesses a moderate to high porosity and a distinctive open to moderately packed texture. The sand and silt layers locally possess a distinctive orange-brown (under plane polarised light), birefringent clay cement which forms rims upon detrital grains or fills the intergranular porosity. A weak shape alignment of elongate detrital grains parallel to the lamination has also been recorded.

The lamination within Unit B is defined by the variation in the modal proportion of a primary clay matrix and/or orange-brown cement, as well as a slight change in grain size of the sediment (Figure 3). At low magnification the boundaries between the individual laminae are sharp. However, at higher magnifications these boundaries are more gradational in character. The layer at the base of the unit is slightly more coarse-grained and contains angular fragments of orange-brown birefringent clay, opaque minerals and silt; the latter derived from the erosion on the underlying unit. A weakly developed normal grading has also been noted within a number of the laminae, with a fine lag composed of fine to medium sand occurring at the base of the lamina.

Detrital grains are mainly angular to subangular in shape with a low to moderate sphericity and cuspate, concave grain boundaries. Rare subrounded grains have also been noted. The detrital clasts are mainly composed of monocrystalline quartz with subordinate to minor feldspar and lithic fragments. Minor to accessory detrital components include variably altered plagioclase, andesitic or basaltic rock fragments, opaque minerals, pseudomorphs after olivine and/or pyroxene, amphibole, very fine-grained schistose or phyllitic rock, microcline, polycrystalline quartz, felsite, tourmaline, apatite and clinopyroxene. Detrital quartz grains are locally partially enclosed within overgrowths which are interpreted as preserving relict of an earlier cement within the source sandstone.

Unit B is overlain by stratified diamicton (Unit C, Figure 3 and Plate 7a) which is compositionally similar to, and forms part of the same unit present within sample N2594. In this sample the diamicton is composed of alternating layers or lenses of massive diamicton and partially disrupted silty material (Figure 3 and Plate 7). The boundary between the diamicton and the underlying sand and silt is sharp (Plate 7a), but is irregular in form with lobes or flames of sand extending into the overlying diamicton.

The diamicton layers are poorly sorted with an open packed, matrix-supported texture and red-brown clay matrix. The matrix is massive and only very locally possesses a weakly developed plasmic fabric. Clasts included within the diamicton are angular to occasionally subrounded in shape with a low to moderate sphericity. The larger, coarse sand to small pebble-sized clasts are composed of rock fragments including variably altered basalt, fine- to medium-grained quartzose litharenite and fine-grained quartz-arenite (Plate 7b, c and d). The basaltic rock fragments (Plate 7d) were probably derived from the Dinantian Clyde Plateau Volcanic Formation, with the sandstones (Plate 7b and c) from the Swanshaw Sandstone Formation of the Siluro-Devonian

Lanark Group. The larger clasts are locally enclosed within a slightly clay-rich coating which locally possesses a weakly developed skelsepic plasmic fabric. Circular arrangements (Plate 7b and c) and clustering of finer grained detrital clasts have been noted within the diamicton.

The silty layers within the diamicton are composed of originally finely laminated silt, clayey silt and silty clay (Plate 7a and d). This fine-scale lamination has been disrupted due to the variable fluidisation of the clay-poor silt laminae and homogenisation of the sediment within these clay-silt layers. Recognisable deformation structures present include asymmetrical folds and microfaults. The most highly disrupted layer also contains partially included 'clasts' of diamicton and coarser grained sand grains derived from the adjacent diamicton (Plate 7c). These 'clasts' of diamicton are morphologically similar to the till pebbles described by van der Meer (1993). They vary from rounded to elongate in shape and may locally possess distinct 'tails'. Internally these clasts or till pebbles are typically massive (comparable with Type 1 till pebbles of van der Meer, 1993). However, complete or partial circular structures have also been noted.

The sand grains (mainly monocrystalline quartz) incorporated into the silt-clay layers are enclosed within a variably developed hematitic clay coating which is petrographically similar to the fine matrix component of the diamicton. The highly disrupted clay and silt layers also contain angular (broken) and partially rounded fragments of the original laminated clayey silt and silty clay set within a matrix of homogenised silt (mud clasts on Plate 7b and c). Internally these fragments of laminated silt and clay are cut by fine-scale hydrofractures filled by a orange-brown, birefringent clay cutan. These clay-lined hydrofractures appear to be restricted to the silt-clay layers and, at least in part, pre-date the internal disruption of these originally laminated layers. The intensity of disruption and homogenisation of the clay-silt layers is apparently dependant upon the number and thickness of the silt laminae, the latter being more prone to liquefaction.

The lowest silt-clay layer, which occurs at the base of Unit C, is cut by an irregular hydrofracture filled by a distinctive orange-brown clay cutan (Plate 7d). This hydrofracture cross cuts and, therefore, post-dates, microstructures developed during the internal deformation and disruption of the clay-silt layer. The hydrofracture appears to originate from the underlying sand of Unit B. In thin section it can be seen that the clay cutan filling the hydrofracture is compositionally similar to the clay cement developed within the laminated sand and silt.

Collectors Number: EY416. **Registered Number:** N2596. **Location:** Westend Wood sand and gravel quarry. **Lithology:** laminated sand and silty sand immediately below the base of the coarse diamicton.

Description: This thin section is mainly composed of fine-grained sand which possesses a distinctive orange-brown clay cement (Figure 4). The lower part of the thin section, however, is composed of partially fluidised and disrupted, weakly laminated fine silt. This laminated silty unit is cut by two hydrofractures filled by matrix-poor, clean silt with the larger fracture also containing angular to subangular fragments of coal. A late stage clay cutan is also developed within this large hydrofracture. The fracturing event resulted in the brecciation of the adjacent, more clay-rich sediment (Figure 4).

The base of the overlying sand is sharp, possibly erosive in nature. The sand is fine-grained and poorly sorted with an open packed, cement-supported texture (Plate 8). This sand is texturally and compositionally similar to and, therefore, correlated with the sand layers present in samples N2954 and N2595 (compare Plates 8a and 4b) which occur immediately below the stratified diamicton. The cement within the sand is composed of a red-brown to orange-brown (under plane polarised light), strongly birefringent clay. A well-developed plasmic (omnisepic) fabric developed within the clay is distorted around the clastic grains. The variation in the intensity of cementation is apparently related to grain size and packing of the sand. Areas of well-developed

clay cementation correspond to areas with an open to very open packed texture and slightly more coarse-grained. Traces of a later, opaque or hematitic cement have also been recognised within this sandy unit.

Detrital grains range from coarse silt to fine sand in size and are typically angular to subangular in shape with a low sphericity. Subrounded sand grains have also been recognised. The detrital grains are mainly composed of monocrystalline quartz with minor rock fragments and detrital feldspar. Minor to accessory detrital components present include plagioclase, polycrystalline quartz, microcline, opaque minerals, coal, bowlingite/serpentine pseudomorphs after olivine and/or pyroxene, very fine-grained volcanic rock, altered biotite, muscovite/white mica, felsite and mudstone.

The sand unit contains several rounded to irregular, elongate voids which are variably filled by a bright orange-brown (under plane polarised light), strongly birefringent clay cutan (Plate 8). This clay possesses a well developed plasmic fabric which occurs parallel to the margins of the voids and is locally distorted or deformed (Plate 8b). The cutan is similar in appearance to the clay cement of the sand. Consequently, these clay-filled or lined voids are interpreted as representing partially filled water escape conduits (see Section 4.5).

In the lower part of the sand unit is a rounded ‘clast’ or augen of diamicton (c. 12 to 15 mm in diameter) enclosed within tails of variably disrupted laminated silt and clay (Figure 4). The diamicton contains a rounded, low sphericity lithic clast composed of hematised basalt. This augen of diamicton is cut by an irregular fracture filled by an orange-brown, birefringent clay cutan. The diamicton is compositionally similar to that within samples N2594 and N2595. The clay within these tails is fragmented and contained within massive, partially fluidised silt. The weak asymmetry of the tails indicates a sinistral (top to left) sense of rotation within this plane of section.

Collectors Number: EY417. **Registered Number:** N2597. Location: Westend Wood sand and gravel quarry. **Lithology:** deformed laminated sand and silty sand approximately 30 cm below the base of the coarse diamicton.

Description: This thin section is mainly composed of laminated silt, clayey silt and very fine sand with the sedimentary lamination being defined by the slight variation in grain size and modal clay content. The lamination is deformed and variably disrupted by three prominent folds (Figure 5) and associated reverse faults (thrusts) which developed in response to soft sediment deformation.

For ease of description the thin section can be divided into three structural ‘domains’ (Figure 5). The lower part of the thin section is deformed by a recumbent rootless fold as well as a number of silt-filled hydrofractures and flame structures. The sedimentary lamination deformed by the recumbent fold is diffuse, possibly due to the on-set of liquefaction of the silt laminae. The silt-filled hydrofractures cross-cut and, therefore, post-date this fold structure. The recumbent fold is truncated by a marked thrust system which is associated with a 0.2 to 0.5 mm wide zone of imbrication. This thrust is curved in form, becoming steeper adjacent to a thicker layer of fine-grained sand which occurs at the top of the underlying unit. One of the silt-filled hydrofractures links into the thrust with liquefied silt apparently having penetrated along this structure.

The laminated clay, silt and very fine sand above the thrust are deformed by three steeply inclined to subvertical, 3 to 5 cm-scale folds which are separated by moderately dipping reverse faults (Figure 5). The previously described thrust and associated imbrication represents a zone of detachment separating these folded sediments from the underlying unit. In detail, the moderately to steeply dipping reverse faults which separate the folds are relatively diffuse structures and at high magnifications lack any obvious discrete planes of shear. Furthermore, no obvious unistrial

plasmic fabric has been recognised within the clay-rich laminae adjacent to these faults. The style of folding changes across (left to right) the thin section related to the variation in the degree of liquefaction of the silt and fine sand layers, in particular a pale coloured (under plane polarised light), clay-poor silt to very fine sand layer (Figure 5). The structurally highest of these fold structures (fold A on Figure 5) is an asymmetrical tight, moderately to steeply inclined structure with a weakly curved axial surface. The lamination thins rapidly around the hinge of the fold, with the overturned limb being highly attenuated (Figure 5). The silt and fine sand layers deformed by this fold show very little evidence of liquefaction. The overturned, lower limb of this fold is truncated by a prominent reverse fault or thrust. This thrust exhibits a sense of displacement towards the east or south-east.

The second fold structure (Fold B on Figure 5) occurs within the hanging-wall of this thrust. This fold is more upright in form with the lamination being deformed by poorly developed disharmonic minor folds. A marked silt and sand layer thickens around the hinge of the fold and shows clear evidence of having undergone partial liquefaction. A weak sedimentary lamination within this layer is variably overprinted due to the partial homogenisation of the silt during fluidisation. The liquefaction of the silt to very fine sand layer is in marked contrast to the clayey silt within the core of the fold which is deformed by a number of small-scale normal and reverse faults. These faults probably developed as accommodation structures whilst the fold progressively tightened. The over tightening of the fold may have also initiated the fluidisation of the silt to fine sand layer.

The final fold structure within the thin section (Fold C on Figure 5) is more complex in form and shows a greater degree of liquefaction of the silt and very fine sand layers. Although the original lamination can still be recognised it is highly contorted, with rapid changes in the thickness of individual laminae (Figure 5). The overall shape of the fold is similar to an inverted tear-drop and it passes downward and links into the thrust zone which separates the folds from the underlying sediments.

The folded unit is bounded at the top by a marked planar contact/bedding surface with the overlying sediment showing very little evidence of deformation (Figure 5). A weak lamination and cross-lamination can be recognised within this fine sandy unit.

4 Interpretation of microstructures

A wide variety of microtextures and deformation structures have been recognised within the diamicton and underlying sediments. This section deals with the interpretation of these structures and their mode of formation with particular reference to the deposition of the diamicton.

4.1 PLASMIC FABRICS

Plasmic fabrics are only locally developed within the sediments examined from the Carstairs area. This is partially due to the silt and sand dominated nature of these deposits, hence restricting plasmic fabric development. However, weak bedding-parallel to locally oblique foliation (approximately 35° to bedding) may be developed within the silty layers defined by the preferred shape alignment of detrital white mica flakes (e.g. N2593). This type of fabric probably developed during the deposition of the sediment rather that any subsequent deformation event. In

contrast to the silts and sands, the more clay-rich layers locally possess a weak to locally well-developed bedding-parallel S1 plasmic fabric. This fabric probably developed in response to compaction as deposition of the sedimentary sequence continued. In sample N2593, the S1 fabric within an orange-red clay lamina is deformed by a set of micro-scale kinks which yield an apparent sinistral (top to left) sense of shear. These structures are rare and, therefore, suggest that the sediments have, in general, undergone very little if any deformation.

A complex, random to locally circular plasmic fabric is developed within the orange-brown, highly birefringent clay matrix of the open-packed sand unit which occurs immediately below the base of the diamicton. This fabric is distorted around the detrital grains and is petrographically similar to the clay cutan noted lining a number of hydrofractures (see Section 4.4). The complex plasmic fabric developed within the clay cement and cutan is interpreted as being a primary feature, forming during the 'deposition' of the clay.

Plasmic fabrics, including a crude lattisepic and/or a skelsepic plasmic fabric, are only weakly developed within the diamicton. The matrix of this deposit is massive and composed of a red-brown (under plain polarised light) hematitic clay-rich material. The poorly developed nature or apparent absence of a plasmic fabric within the diamicton may, at least in part, masked by the hematitic staining of the clay. In general, the presence of hematite and/or carbonate within the matrix of a diamicton will result in the masking of a plasmic fabric due to the strong body colour and high birefringence (respectively) of these phases.

4.2 ORIGIN OF CIRCULAR STRUCTURES WITHIN DIAMICTONS

Circular and galaxy structures present within diamictons are thought to be indicative of subglacial deformation (van der Meer, 1993, 1997). These structures comprise a circular arrangement of finer grained (sand grade or below) clasts around a central 'core stone' formed by a larger detrital grain (Plates 9 and 10). This core stone acted as a node for rotation during deformation. In cases were the core stone is absent, van der Meer (1993) suggested that the central area may have been drier and thus representing a harder spot within the deforming till bed. Van der Meer (1997) suggested that subglacially deformed diamictons (tills) are made up of rotational elements or wheels, consisting of a nucleus alone or a nucleus with spiralling arms (galaxy structures) of finer grains. The presence of such structures is thought to record clast mobility within the deforming subglacial till, with finer grains moving from one wheel to the next (van der Meer, 1997, figs. 2 and 3).

Circular and arcuate aggregates or arrangements of finer grained clasts, with or without a core stone, are present within the diamicton examined from the Carstairs area (Plates 9 and 10). The lack of asymmetry and completely circular nature of these micromorphological features suggests that the clastic grains were free to rotate through more than 360°. Importantly, the bulk of the diamicton is massive, and displays very little evidence of solid-state deformation. The field relationships and sedimentology of the associated glaciofluvial sandur deposits clearly indicate that this diamicton was not deposited in a subglacial environment. Thomas and Montague (1997) interpreted the diamictons within this sequence as supra- to pro-glacial mass flow deposits. Furthermore, these mass flow deposits do not show any evidence of having been subsequently over-ridden by ice. Consequently, the presence of circular and/or galaxy structures in diamictons can not be used as an indicator of subglacial deformation.

The simplest interpretation of circular structures is that they record rotational movement within the diamicton (*cf.* van der Meer, 1993). However, in rocks (e.g. schists and mylonites) any deformation which involves a strong component of simple shear (i.e. rotation) results in the development of asymmetrical structures, such as porphyroclast systems, pressure shadows or

tails developed upon rotated porphyroblasts and S-C fabrics (Vernon, 1989; Passchier and Trouw, 1996). Importantly, these structures are typically associated with very high shear strains encountered within ductile shear zones (e.g. Eilrig Shear Zone, Phillips *et al*., 1993). The micromorphology of the galaxy textures and skelsepic plasmic fabrics are more reminiscent of coated clastic grains present within undeformed sedimentary rocks. These coated grains may also posses a concentric structure which developed as material adhered to the surface of a freely rotating clast in the sedimentary environment. Consequently, the physical properties of a diamicton must provide the major controlling factor on the formation of circular and galaxy structures, in particular allowing clast rotation through more than 360°.

An important factor, which appears to have been, over looked in the models of van der Meer (1993, 1997) is that water saturation can lead to the liquefaction of sediment, including diamictons. Subglacial tills and mass-flow deposits are believed to be saturated with water during their deposition (Boulton and Hindmarsh, 1987; Clarke, 1987; Alley, 1989; Boulton, 1996). A high water content and/or pressure will result in a weakening of electrostatic bonds and increase in the distance between the component clastic grains. This leads to a decrease in both the cohesion and frictional strength, and an increase in the volume or dilation of the sediment (Alley, 1989). The dilation of the sediment will, in effect, allow the component grains to move past each other more easily during shear (Murray and Dowdeswell, 1992) and rotate freely in three dimensions. As the pore water content and/or pressure falls below a critical point the dilated sediment will collapse (i.e. solidify) leading to an increase in shear strength and allowing solid state deformation to occur. An important point to be made here is that a liquefied granular material will not take up deformation, its response to any applied stress will be to ‘flow’.

Consequently, an alternative model for the formation of circular or galaxy structures and associated skelsepic plasmic fabrics within diamictons is that they developed during highly plastic/fluid flow rather than solid-state deformation. The variable preservation of these circular textures and the occurrence of such structures without a ‘core stone’ may reflect the transitory nature of the rotating ‘eddy currents’ within the actively flowing matrix of the diamicton. Once the eddy or vortex has dissipated the driving force maintaining the integrity of the circular and/or galaxy structure will be lost, and it will begin to be fragmented and subsequently overprinted.

If correct, this new model for the formation of circular and galaxy structures will have considerable implications for the way in which we view conditions during till deposition and glacier/ice sheet movement.

4.3 EVIDENCE FOR FLUIDISATION AND SEDIMENT MIXING WITHIN THE DIAMICTON

The diamicton (N2594, N2595) sampled from the Carstairs Quaternary sequence possesses a well-developed, streaky-looking stratification consisting of alternating layers or bands of coarse-grained, poorly sorted, matrix-supported diamicton and laminated silt and clay (Figures 2 and 3). The laminated silt and clay layers are lithologically similar to, and were probably derived from similar units present within the underlying sedimentary sequence. Internally the silt-clay layers show varying degrees of deformation and fluidisation of the silt laminae. Microtextures recognised within this stratified diamicton may be interpreted as recording initial soft-sediment deformation (Plates 9, 10 and 11), followed by the onset of mixing of the diamicton and silt-clay layers.

Soft-sediment deformation of the silt-clay layers resulted in the development of asymmetrical to disharmonic folds (Plate 10a), flame structures, diffuse microfaults, fractures and/or shears which deform bedding and an earlier developed bedding-parallel S1 plasmic fabric. Stretching of

the clay-silt layer also occurred leading to necking and eventual boudinage of the more highly deformed layers.

Although the silt laminae have undergone varying degrees of liquefaction (Plates 9d and 10b) the clay-silt layers have, in general, remained relatively coherent. The boundaries between the layers are sharp, but vary from planar, to irregular, to flame-like or cuspate in form (Plate 9a, b and c). The presence of circular structures within the cuspate bed forms (Plate 9a and c) may be used to suggest that deformation of the silt-clay layers accompanied flow within the fluidised matrix of the diamicton. Instability along the boundaries between the layers, caused by the difference in rheological properties of the silt-clay and adjacent diamicton, would have resulted in the initial formation of these cusp and flame structures. Continued movement ('flow') resulted in the tightening and eventual detachment of these structures leading to the formation of isolated fragments of diamicton (Type 1 till pebbles of van der Meer, 1993) (Plates 10b, c and d) within the clay-silt layers and ribbons of clay within the adjacent diamicton (*cf.* sand ball development during soft-sediment deformation). Some of the till pebbles posses distinct tails (Plate 11d), formed during either the initial detachment of the pebble from the parent diamicton or subsequent rotation of the clast.

The presence of included detrital grains, derived from the adjacent diamicton (Plates 9b, 10c, 10d, 11a and 11c), within the silt-clay is interpreted as recording the transfer of material between the diamicton and silt-clay layers. These included grains, in particular the larger lithic clasts, are locally enclosed within a variably developed coating which is similar in composition to the matrix of the diamicton (Plate 11c). During these initial stages of mixing the integrity of the silt-clay layers was maintained; possibly due to the rheological contrasts between the liquefied diamicton and still partially solid silt-clay layers. Only as the intensity of fluidisation and accompanying internal disruption of the silt-clay units reached a critical point did these fine-grained layers begin to loose their coherence, becoming more diffuse in nature. The rate of liquefaction of the silt-clay layers is believed to be largely controlled by the number and thickness of the silt laminae. The fluidisation of the silt layers resulted in the development of circular, arcuate and occasional galaxy structures defined by the arrangement of included grains derived from the adjacent diamicton (Plates 10b and 11a).

4.4 HYDROFRACTURING

Hydrofractures are the main type of deformation structure present within the sedimentary sequence exposed below the diamicton. Two main textural varieties of hydrofractures have been recognised: (1) subvertical to horizontal matrix-poor sand or coarse silt-filled fractures (N2593, N2596) (Plate 3a); and (2) fine-scale, irregular to wispy-looking structures filled by a distinctive orange-brown, birefringent clay cutan (N2593, N2594. N2595).

The sand- to silt-filled hydrofractures are best developed in sample N2593 where they form a network of subvertical and horizontal structures which are fed by one main conduit (Figure 1 and Plate 3c). The sand- to silt-fill of these fractures is graded becoming finer grained upward, accompanied by a narrowing of the hydrofractures. Brecciation of the sediment adjacent to these fractures is relatively restricted, with only occasional fragments of 'wall rock' included within the fluidised sand-fill to the hydrofractures. More complex fracture patterns (including sigmoidal, en-echelon tension fissures) are also present towards the termination of the fracture networks. The orientation of the hydrofractures is possibly related to the modal proportion of clay in the 'host' sediment. The presence of clay laminae (1.5 to 2.0 mm thick) within the sand- to silt-dominated sequence resulted in the retardation of upward migration of water and fluidised sand (see Plate 3b). The pressurised liquefied sand was then forced to spread out laterally parallel to bedding along the base of the overlying clay-rich layer. However, when the cohesive

strength of the clay layer is exceeded, for example due to an increase in pore water pressure, the upward propagation of the hydrofractures and escape of fluidised sand would be re-initiated (see Plate 3b). Hydrofracturing of the clay-rich layers may be preceded by the upward 'doming' or warping of the layer. This apparently occurred due to the injection of fluidised sand, leading to an increase in volume of the sediment immediately below the clay layer.

Similar matrix-poor sand-filled hydrofractures are also present deforming a laminated silty unit at the base of sample in N2596 (see Fig. 4). The larger of these fractures also contains fragments of coal and a late-stage fill or clay cutan.

The second group of hydrofractures are distinguished by the presence of an orange-brown, highly birefringent clay cutan (see Plates 5c and 7d). In the stratified diamicton these clay-filled fractures show a range of relationships to soft-sediment deformation structures, fluidisation and mixing of the clay-silt layers with the host diamicton. In samples N2594 and N2595 the clay cutan occurs as broken fragments or filling very fine fractures within clasts of laminated silt and clay within the more highly disrupted clay-silt layers. This relationship indicates that hydrofracturing occurred prior to the fragmentation of the clay and liquefaction of the interlaminated silt. In contrast, an irregular clay-filled hydrofracture within sample N2595 cross-cuts and, therefore, post-dates, all the microstructures associated with internal deformation and disruption of the clay-silt layers (Plate 7d). The host diamicton may also contain irregular to wispy-looking clay-lined fractures, which probably represent fluid pathways which were active during the dewatering of the mass flow deposit. Consequently, there are several generations of clay-filled hydrofractures within these deposits.

4.5 ORIGIN OF THE 'CEMENT-SUPPORTED' SAND UNIT

The coarse diamicton within the Carstairs sequence is separated from the underlying sand dominated glacifluvial sediments by a distinctive red coloured, 10 to 20 cm thick sand layer (Plate 1a). In thin section, this finely laminated to massive, fine- to medium-grained sand possesses a distinctive open to very open packed, 'cement-supported' texture (N2593; N2594; N2595). The base of this sandy unit clearly truncates bedding and erodes into the underlying laminated silt, silty sand and/or sand. The upper boundary between the sand and the overlying diamicton is sharp, but may be modified during the fluidisation of the sand.

In detail, the lamination (where present) within the sand is defined not only by a variation in grain size, but also by the variation in the modal proportions of a orange-brown clay cement (Plate 4b). This highly birefringent clay is petrographically similar to the clay cutan present within the hydrofractures (see Section 4.4). The random to locally circular plasmic fabric developed within the clay cement is distorted around the clastic grains. This distortion is apparently a primary feature and probably occurred during the formation of the cement. In the sand laminae in which this cement is less well developed, the clay was noted lining or locally filling intergranular pore spaces.

The 'cement-supported' texture of the sand means that very few of the clastic grains are in contact. This microtexture suggests that cementation occurred when the sand was in a dilated, probably fluidised, state. However, fluidisation of the sand has not resulted in the disruption and overprinting of the lamination present within this unit. Consequently, it is unlikely that the lamination is a primary sedimentary feature, but developed during fluidisation and cementation. Rather than being a part of the primary sedimentary sequence it is possibly that this sand unit was injected along the boundary between the diamicton and underlying sand- and silt-dominated sequence. This interpretation is supported by the fact that the sandy unit clearly cross-cuts the stratification within the diamicton and bedding within the underlying sediments. Furthermore,

the basal part of the diamicton is cut by hydrofractures which are filled by clean sand which was derived from the laminated sand unit. Therefore, fluidisation and injection of the sand, coupled with hydrofracturing of the diamicton must have, at least in part, post-dated the deposition of this very coarse grained deposit. This conclusion is supported by the presence of a clast or augen of diamicton within the sand, which was detached from the overlying diamicton during injection. This sample also contains several rounded to irregular water-escape conduits which are filled by a strongly birefringent, orange-brown clay cutan, similar in appearance to the clay cement of the sand (Plate 8). These features probably developed as cementation of the sand led to a decrease in porosity and permeability, resulting in fluid flow being concentrated into discrete conduits during the later stages of sediment dewatering.

4.6 SOFT-SEDIMENT DEFORMATION

In general the sand-dominated glaciofluvial sequence examined during this present study is undeformed. Soft-sediment deformation, where present, is largely restricted to a c. 10 cm wide zone which occurs approximately 30 cm below the base of the diamicton. The top of this folded and faulted layer is bounded by a planar bedding surface, with the overlying sediment showing very little evidence of deformation (see Figure 5).

The sedimentary lamination within this layer is deformed and variably disrupted by a number of variably disharmonic, upright to recumbent folds as well as associated minor reverse faults and water-escape structures (sample N2597). The sense of asymmetry of the folds and displacement on the associated thrust faults records a sense of movement towards the south-eastern quadrant. The style of folding varies with respect to the degree of liquefaction of the silt and fine sand laminae. Fluidisation of the silt and sand apparently occurred in response to the tightening of the earlier developed folds as deformation progressed. In contrast, tightening of the folds resulted in minor faulting of the more cohesive clay and silty clay laminae; the small-scale normal and reverse faults within the cores of the folds, therefore, represent accommodation structures.

It is possible that soft-sediment deformation simply occurred in response to the vertical loading and compaction of the sedimentary sequence. This deformation was partitioned into the more silty horizon with the adjacent, more massive, sands showing very little or no evidence of disruption apart from localised hydrofracturing. The sense of asymmetry of the folds and off-set on the thrust faults clearly indicate that there was probably a significant component of lateral displacement (towards the south-east) to this deformation. Consequently, simple loading of the sediments is unlikely to have been the driving force. An alternative mechanism for inducing soft-sediment deformation within silty horizons may have been the deposition of the mass flow deposit, represented by the very coarse diamicton. Thomas and Montague (1997) suggested this laterally extensive deposit formed due to catastrophic slumping of debris into the margin of the ice-dammed lake which had developed between the Highlands and Southern Uplands ice. The emplacement of this diamicton, which contains large boulders of basalt (1.5 m in diameter), may have triggered soft-sediment deformation within the underlying, possibly water-saturated, sediments. The sand-dominated nature of much of this sequence meant that deformation was partitioned into the weaker silty horizons. This may have accompanied hydrofracturing within the sandier units (see section 4.4.).

5 Micromorphological evidence for conditions during emplacement of mass flow deposits

The very coarse diamicton examined during this study and that of Thomas and Montague (1997) clearly represents a significant event during the deposition of the Carstairs glaciofluvial sequence. Thomas and Montague (1997) argued that the very coarse material within the diamicton originated as supraglacial debris contained within a medial moraine, derived from an exposed nunatak in the Tinto Hills to the south. The boulders within the diamicton, are however, mainly composed of Carboniferous basalt rather than Siluro-Devonian dacite or rhyolite. No Carboniferous lavas are exposed in the Tinto Hills. Consequently, the original source of this basaltic detritus may have lay to the north or west, rather than the south as suggested by Thomas and Montague (1997). A northerly or westerly source of the detritus is possible due to the common occurrence of sandstone fragments, which are lithologically similar to the Swanshaw Sandstone Formation (Lanark Group), within the matrix of the diamicton.

Micromorphological analysis of the diamicton and the underlying sediments has confirmed field observations that even though the deposition of this extremely coarse diamicton represents a significant event (*c.f.* Thomas and Montague, 1997) the underlying sediments show very little evidence of deformation or disturbance. The emplacement of the diamicton, which contains large boulders,1.5 m in diameter, is thought to have triggered soft-sediment within the underlying, probably water-saturated, sediments. However, deformation is restricted to minor folding, faulting and the formation of associated water escape structures within a silty horizon approximately 30 cm below the base of the diamicton. The sense of asymmetry of the folds and displacement on the thrust faults yields a transport direction towards the south or south-east, i.e. consistent with a northerly to westerly source for the coarse detritus.

In contrast to the silty horizon, the overlying sands are relatively undeformed. The only evidence of disturbance is the presence of sand and silt-filled hydrofractures. In general, they form a network of subvertical and horizontal structures which are fed by a main conduit. The presence of clay laminae within the sand-dominated sequence resulted in the retardation of upward migration of water/fluidised sand. This resulted in the lateral spreading of the liquefied material until the cohesive strength of the clay layer was exceeded and upward water-escape was reinstated.

The overlying diamicton contains micromorphological evidence of having been emplaced in a liquefied state, supporting the contention of Thomas and Montague (1997) that it is a very coarse mass-flow deposit. Circular and galaxy structures, as well as the associated skelsepic plasmic fabrics present within the diamicton are here interpreted has having developed in response to highly plastic or fluid flow, rather than solid-state deformation. However, solid-state deformation appears to have been restricted to the localised development of a weak lattisepic plasmic fabric within the matrix of the diamicton. The slightly stronger skelsepic plasmic fabrics are spatially related to the circular textures and are, therefore, believed to be linked to the formation of these structures. The variable preservation of the circular textures is considered to reflect the transitory nature of the rotating ‘eddy currents’ within the actively flowing matrix of the diamicton. Once the ‘eddy’ or ‘vortex’ has dissipated the driving force maintaining the integrity of the galaxy structure will be lost and it will begin to ‘fragment’; the latter leads to the presence of arcuate alignments of clastic grains. As the pore water content and/or pressure falls below a critical point the dilated matrix of the diamicton will collapse (solidify) leading to an increase in shear strength and allowing solid-state deformation to occur. The presence of circular textures within a mass flow deposit, which does not also show any evidence of having been subsequently over-ridden by ice, means that such structures cannot be used as indicators of subglacial deformation (van der Meer, 1993).

The stratified base of the diamicton possesses microtextures within the silt and clay layers which are consistent with initial soft-sediment deformation, followed by the onset of liquefaction and mixing of these layers with the host diamicton. The progressive formation and detachment of small-scale cuspate lobes of diamicton resulted in the formation of type 1 till pebbles (van der Meer, 1993) within the silt and clay layers. Included grains, derived from the adjacent diamicton, record the transfer of material between the diamicton and silt-clay layers. However, during the emplacement of the diamicton the integrity of the silt-clay layers was, in general, maintained, possibly due to the rheological contrasts between the liquefied diamicton and partially solid silt-clay layers. Only as the intensity of fluidisation and disruption of the silt-clay units reached a critical point did these fine-grained layers begin to become more diffuse in nature and mix with the host sediment.

One important feature which remains to be explained is the lack of any major disturbance of the underlying sediments associated with the emplacement of the diamicton. As previously stated, this mass flow deposit contains very large boulders which, in theory, should have impacted with and distorted the underlying sediment during transport. Such features are not present in the section examined during this study (see Plate 1). In this outcrop, the coarse diamicton is separated from the underlying sand dominated glacifluvial sediments by a 10 to 20 cm thick sand layer (Plate 1a). The ‘cement-supported’ texture of the sand indicates that cementation occurred when it was in a dilated, probably fluidised, state. This sand layer clearly cross-cuts bedding in the underlying sediments as well as truncating the stratification within the basal part of the overlying diamicton. Both upper and lower boundaries to the layer are sharp, but may have locally been modified during the fluidisation of the sand. Consequently, rather than being a part of the primary sedimentary sequence, it is suggested that the sand unit was injected along the boundary between the diamicton and underlying sedimentary sequence. Injection of the fluidised sand accompanied hydrofracturing at the base of the diamicton. Therefore, fluidisation and injection of the sand, coupled with hydrofracturing of the diamicton must have, at least in part, post-dated the deposition of this very coarse-grained deposit. However, it is possible that this highly fluidised sand layer may have initially developed during the deposition of the diamicton. The development of a super-fluidised sand layer beneath the diamicton would have assisted in the emplacement of this mass flow deposit. The liquefied sand is compositionally similar to and was probably derived from the underlying water-saturated sediments. The upper parts of this sedimentary sequence may have liquefied in response to either the initial trigger generating this mass flow deposit, or the early stages of transport of this material across the glacifluvial sediments. This super-fluidised layer in theory could have protected or ‘cushioned’ the underlying sediments from disturbance as the stresses generated by the incoming of the diamicton would not be transmitted through this water-rich zone. Furthermore, the large boulders may have travelled in suspension (‘floating’) within the liquefied diamicton rather than by saltation. The cross-cutting relationships displayed by the super-fluidised layer and hydrofracturing of the diamicton, probably represent late-stage movement of the water-rich sand during the dewatering and solidification of the diamicton. Cementation of the sand probably occurred at this stage whilst the sand was still in a dilated state. Dilation of the sand could have been maintained by: (a) the retardation of water escape from the sand by the presence of the low-permeability of the diamicton; (b) an increase in pore water pressure as the diamicton ‘sank’ onto its bed; or (c) a combination of both processes. As cementation and dewatering continued, water-escape was concentrated into discrete conduits and/or small-scale hydrofractures which later became filled with a clay cutan.

6 Conclusions

A number of conclusions can be made concerning the origin and micromorphology of the Quaternary sediments associated with the Carstairs Eskers:

- The sand-dominated sequence exposed at the northeastern end of the northern pit of Westend quarry form the distal parts of a fluvioglacial (sandur) sequence (Thomas and Montague, 1997).

- The extremely coarse, massive diamicton present within the sequence represents a major mass flow deposit (*cf.* Thomas and Montague 1997). However, the emplacement of this unit resulted in very little disturbance or deformation of the underlying sediments.

- Boulders within the diamicton are mainly composed of Carboniferous basalt rather than Siluro-Devonian dacite or rhyolite suggested by Thomas and Montague (1997). No Carboniferous lavas are exposed in the Tinto Hills. The original source of this basaltic detritus is could also have lay to the north or west and, therefore, have been transported by Highland ice.

- Plasmic fabrics are only locally developed within the sediments. Bedding-parallel plasmic fabrics present within the more clay-rich sediments probably developed as a result of loading during continued deposition of the sediment sequence, rather than subsequent deformation. Weakly developed lattisepic and skelsepic plasmic fabrics present within the diamicton may be partially masked by the hematitic stain within the matrix of this sediment.

- Circular and galaxy structures present within the mass flow deposit are interpreted as recording rotation associated with fluidisation of the matrix of the diamicton rather than subglacial deformation as suggested by van der Meer (1993, 1997). The variable preservation of these textures is thought to reflect the transitory nature of ‘eddy currents’ or vortices within the actively flowing diamicton.

- Microtextures recognised within this stratified diamicton may be interpreted as recording initial soft-sediment deformation, followed by the onset of mixing of the diamicton and silt-clay layers.

- Hydrofractures are the main type of deformation structure present within the sedimentary sequence exposed below the diamicton. Two main textural varieties have been recognised: (1) subvertical to horizontal matrix-poor sand and silt-filled structures; and (2) fine, irregular to wispy-looking fractures filled by an orange-brown clay cutan.

- In general the sand dominated sequence is undeformed. Soft-sediment deformation (folding, faulting), where present, is largely restricted to a *c*. 10 cm wide, laminated, silty horizon. The sense of asymmetry of the folds and off-set on the thrust faults is consistent with a south-easterly directed sense of movement. Soft-sediment deformation is thought to have accompanied deposition of the mass-flow deposit.

- The diamicton is separated from the underlying sediments by a distinctive dilated, cement-supported sand. This unit is interpreted as recording the presence of a super-fluidised sand layer which formed beneath the diamicton during deposition, assisting the emplacement of this mass-flow deposit and protecting the underlying sediments from disturbance.

Glossary

Micromorphology – A term used to describe the study of unconsolidated glacial sediments in thin section using a petrological microscope.

Plasmic fabric – The optical arrangement of high birefringent clay plasma/domains which are visible under crossed polarised light using a petrological microscope.

Unistrial plasmic fabric – A planar plasmic fabric defined by relatively continuous domains which is typically observed defining discrete shears (van der Meer, 1993).

Skelsepic plasmic fabric – A plasmic fabric in which the orientated domains occur parallel to the surface of large grains (van der Meer, 1993).

Lattisepic plasmic fabric – A plasmic fabric defined by short orientated domains in two perpendicular directions (van der Meer, 1993).

Omnisepic plasmic fabric – A plasmic fabric in which all the domains have been reoriented (van der Meer, 1993).

Grain size – (a) clay < 0.0039 mm in size; (b) silt, 0.0039 to 0.0625 mm in size; (c) fine sand, 0.0625 to 0.25 mm in size; (d) medium sand, 0.25 to 0.5 mm in size; (e) coarse sand, 0.5 to 1.0 mm in size; (f) very coarse sand, 1.0 to 2.0 mm in size; (g) granules 2.0 to 4.0 mm in size; (h) pebbles 4.0 to 64 mm in size.

Rounded – Describes the smoothness of the surface of a grain. The terms well-rounded, rounded, subrounded, subangular, angular, very angular are used to describe the increasingly angular/irregular/rough nature of the surface of detrital grains.

Sphericity – Describes how closely a detrital grain approximates to a sphere. The terms low sphericity, moderate sphericity and high sphericity are used to describe how spherical (ball-like) the detrital grains are.

Sorting – Well sorted describes a deposit in which all the detrital grains are of approximately uniform size. In reality most fragmentary deposits contain a range of grain sizes and can be described as moderately sorted, poorly sorted or in extreme cases unsorted.

Packing – Describes, as the term suggests, how closely the individual detrital grains are packed together within a fragmentary deposit. The term closely packed is used where all the grains are in contact and there is very little obvious matrix or cement; moderately packed and open packed are used with an increase in the porosity, matrix and/or cement.

Clast- supported – Describes a fragmentary deposit where all the detrital grains are in contact.

Clay cutan – a modified texture, structure or fabric of a unconsolidated material (e.g. soil) caused by the concentration of optically aligned, highly birefringent clay plasma.

Matrix-supported – Describes a fragmentary deposit where the detrital grains are, to varying degrees, isolated/supported within a finer grained matrix.

Cement-supported – Describes a fragmentary deposit where the detrital grains are, to varying degrees, isolated/supported within the cement.

Cement – The material bonding the fragments of clastic sedimentary rocks together and which was precipitated between the grains after deposition.

Porosity – The volume of voids expressed as a percentage of the total volume of the sediment or sedimentary rock.

Matrix – Material, usually clay minerals or micas, forming a bonding substance to grains in a clastic sedimentary rock. The matrix material was deposited with the other grains or developed authogenically by diagenesis or slight metamorphism. Also used more generally for finer grained material in any rock in which large components are set.

Detritus – A general term for fragmentary material, such as gravel, sand, clay, worn from rock by disintegration. Detrital grains in clastic sediments or sedimentary rocks may be composed of single mineral grains (e.g. monocrystalline quartz, plagioclase), polycrystalline mineral grains (e.g. polycrystalline quartz) or lithic fragments including sedimentary, igneous and metamorphic rock fragments.

References

Most of the references listed below are held in the Library of the British Geological Survey at Keyworth, Nottingham. Copies of the references may be purchased from the Library subject to the current copyright legislation.

ALLEY, R. B. 1989. Water-pressure coupling of sliding and bed deformation. *Journal of Glaciology*. **35,** 108-139.

BENNETT, M. & GLASSER, N. 1995. Process, bar morphology, and sedimentary structures on braided outwash fans, northeast Gulf of Alaska. *In* JOPLING, A. V. & MCDONALD, B. C. (eds) *Glaciofluivial and Glaciolacustrine Sedimentation. Special Publication of the Society of Economic Palaeontologists and Mineralogists.* **23,** 193-222.

BOULTON, G. S. 1972. Modern Artic glaciers as a depositional model for former ice-sheets. *Journal of the Geological Society of London*. **128,** 361-393.

BOULTON, G. S. 1996. The origin of till sequences by subglacial sediment deformation beneath mid-latitude ice sheets. *Annals of Glaciology*. **22,** 75-84.

BOULTON, G. S. & HINDMARSH, R. C. A. 1987. Sediment deformation beneath glaciers: rheology and geological consequences. *Journal of Geophysical Research*. **92,** 9059-9082.

CHARLESWORTH, J. K. 1926. The Readvance, marginal kame-moraines of the south Scotland and some later stages of retreat. *Transactions of the Royal Society of Edinburgh*. **55,** 25-50.

CLARKE, P. U. 1987. Subglacial sediment dispersal and till composition. Journal of Geology. **95,** 265-287.

GREGORY, J. W. 1915. The kames of Carstairs. *Scottish Geographical Magazine*. **31,** 465-477.

LAXTON, J. L. & NICKLESS, E. F. P. 1980. *The sand and gravel resources of the country around Lanark, Strathclyde Region. Description of 1:25,000 sheet NS94 and part of NS84*. Mineral Assessment Report of the Institute of Geological Sciences. **49**.

MCLELLAN, A. G. 1969. The last glaciation and deglaciation of central Lanarkshire. *Scottish Journal of Geology*. **5,** 248-268.

MENZIES, J. 2000. Micromorphological analyses of microfabrics and microstructures indicative of deformation processes in glacial sediments. *In* Maltman, A. J., Hubbard, B. & Hambrey, J. M. (eds) *Deformation of Glacial Materials*. *Geological Society, London, Special Publication*. **176,** 245-257.

MURRAY, T. & DOWDESWELL, J. A. 1992. Water throughflow and the physical effects of deformation of sedimentary glacier beds. *Journal of Geophysical Research*. **97,** 8993-9002.

OSTRY, R. C. & DEANE, R. E. 1963. Microfabric analyses of till. *Geological Society of America Bulletin*. **74,** 165-168.

PASSCHIER, C. W. & TROUW, R. A. J. 1996. *Microtectonics*. Springer.

PHILLIPS, E. R., CLARK, G. C. & SMITH, D. I. 1993. Mineralogy, petrology and microfabric analysis of the Eilrig Shear Zone, Fort Augustus, Scotland. *Scottish Journal of Geology*. **29,** 143-158.

SERET, G. 1993. Microstructures in thin sections of several kinds of till. *Quaternary International*. **18,** 97-101.

SISSONS, J. B. 1961. The central and eastern parts of the Lammermuir - Stranraer moraine. *Geological Magazine*. **98,** 380-392.

THOMAS, G. S. P. & MONTAGUE, E. 1997. The morphology, stratigraphy and sedimentology of the Carstairs Esker, Scotland, U.K. *Quaternary Science Reviews*. **16,** 661-674.

VAN DER MEER, J. J. M. 1987. Micromorphology of glacial sediments as a tool in distinguishing genetic varieties of till. In *INQUA Till Symposium, Finland 1985*. KUJANSUU, R. & SAARNISTO, M (editors). Geological Survey of Finland, Special Paper **3,** 77-89.

VAN DER MEER, J. J. M. & LABAN, C. 1990. Micromorphology of some North Sea till samples, a pilot study. *Journal of Quaternary Science*. **5,** 95-101.

VAN DER MEER, J. J. M., RABASSA, J. O. & EVENSON, E. B. 1992. Micromorphological aspects of glaciolacustrine sediments in northern Patagonia, Argentina. *Journal of Quaternary Science*. **7,** 31-44.

VAN DER MEER, J. J. M. 1993. Microscopic evidence of subglacial deformation. *Quaternary Science Reviews*. **12,** 553-587.

VAN DER MEER, J. J. M. & VEGERS, A. L. L. M. 1994. The micromorphological character of the Ballycroneen Formation (Irish Sea Till): a first assessment. *In* WARREN & CROOT (eds.) *Formation and Deformation of Glacial Deposits*. Balkema, Rotterdam. 39-49.

VERNON, R. H. 1989. Porphyroblast-matrix microstructural relationships: recent approaches and problems. *In* DALY et al. (eds). *Evolution of metamorphic belts.* Geological Society of London Special Publication. **43,** 83-102.

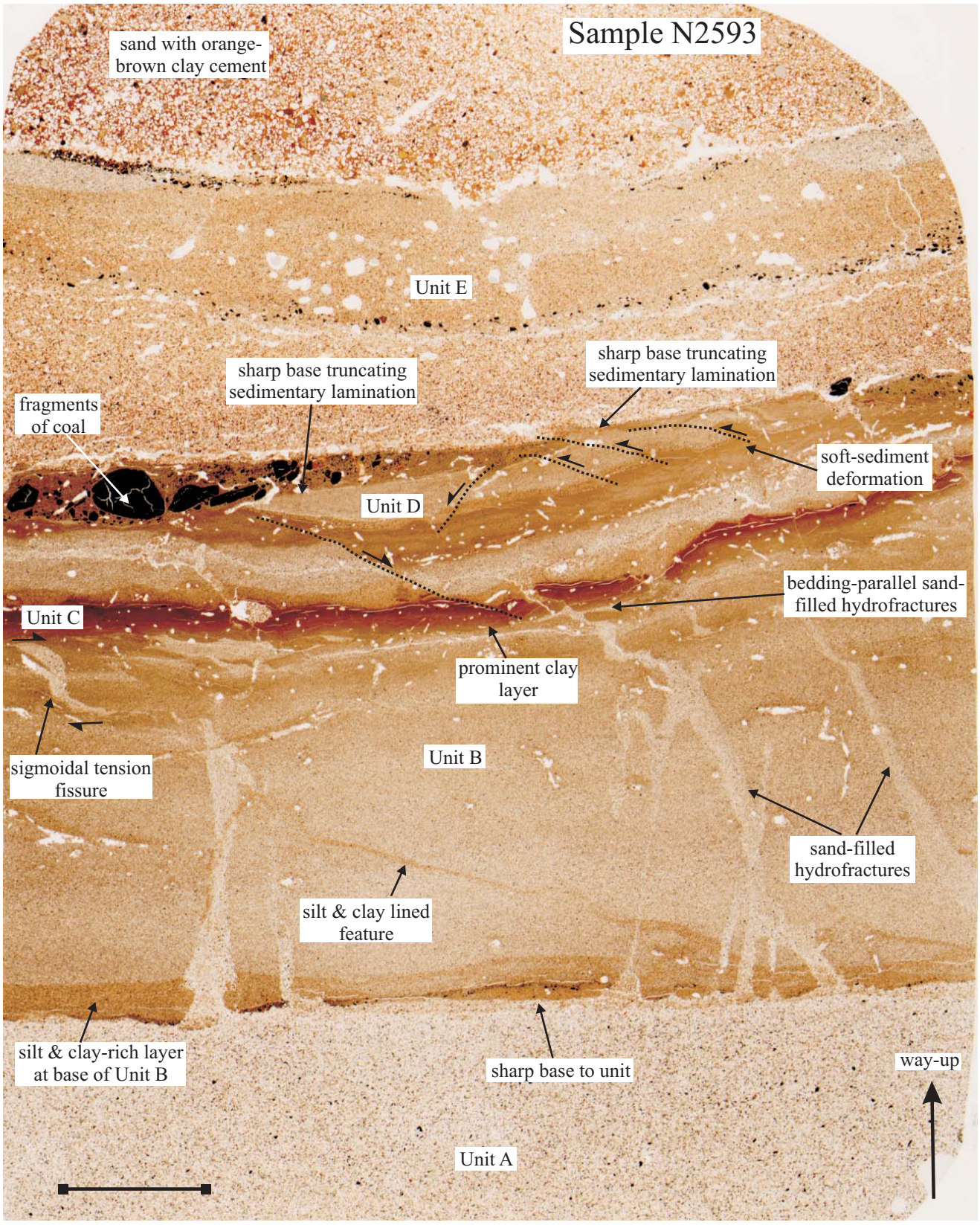

Figure 1. Annotated scanned image of the large format thin section taken from sample N2593 (see text for details). Scale bar = 10 mm.

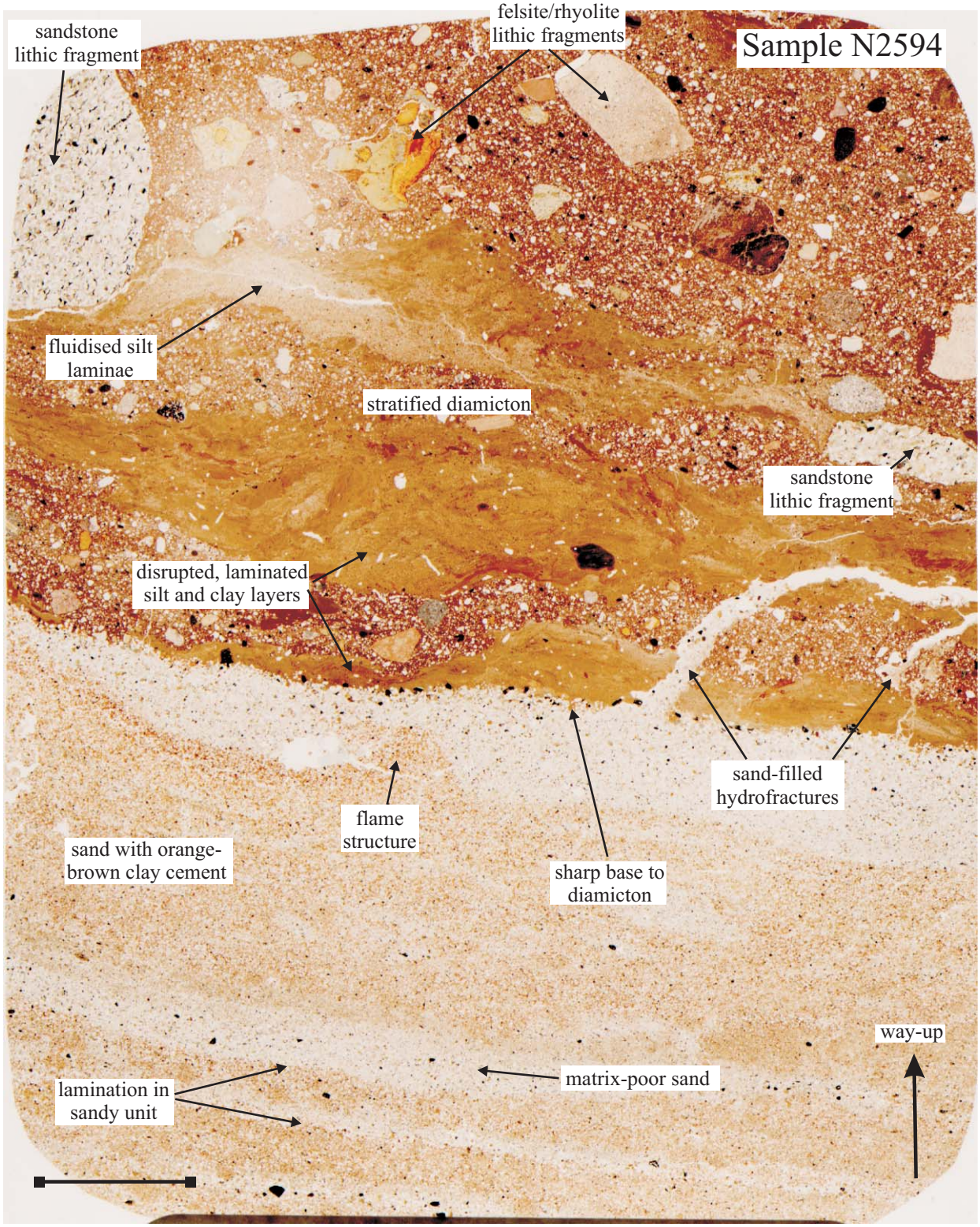

Figure 2. Annotated scanned image of the large format thin section taken from sample N2594 (see text for details). Scale bar = 10 mm.

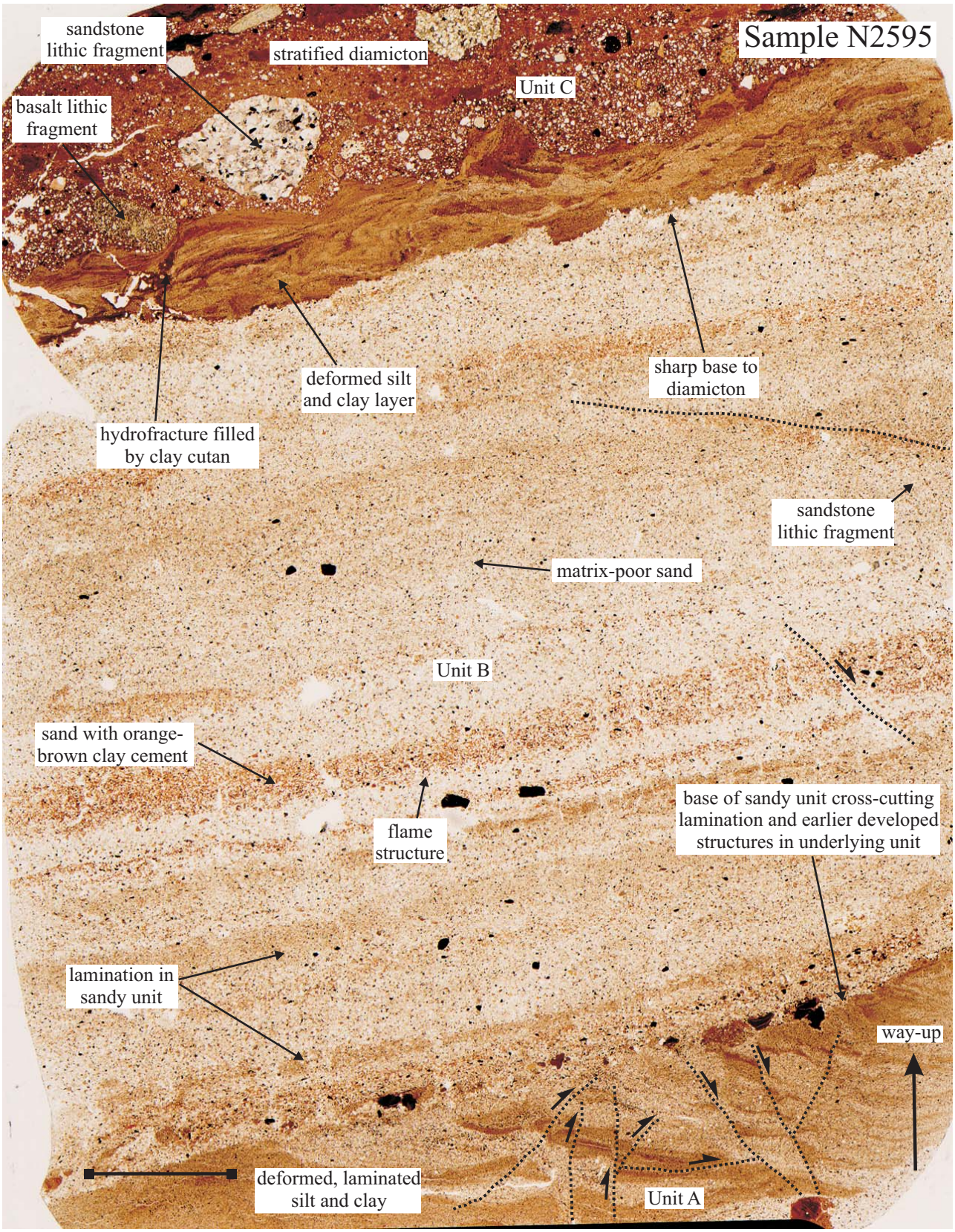

Figure 3. Annotated scanned image of the large format thin section taken from sample N2595 (see text for details). Scale bar = 10 mm.

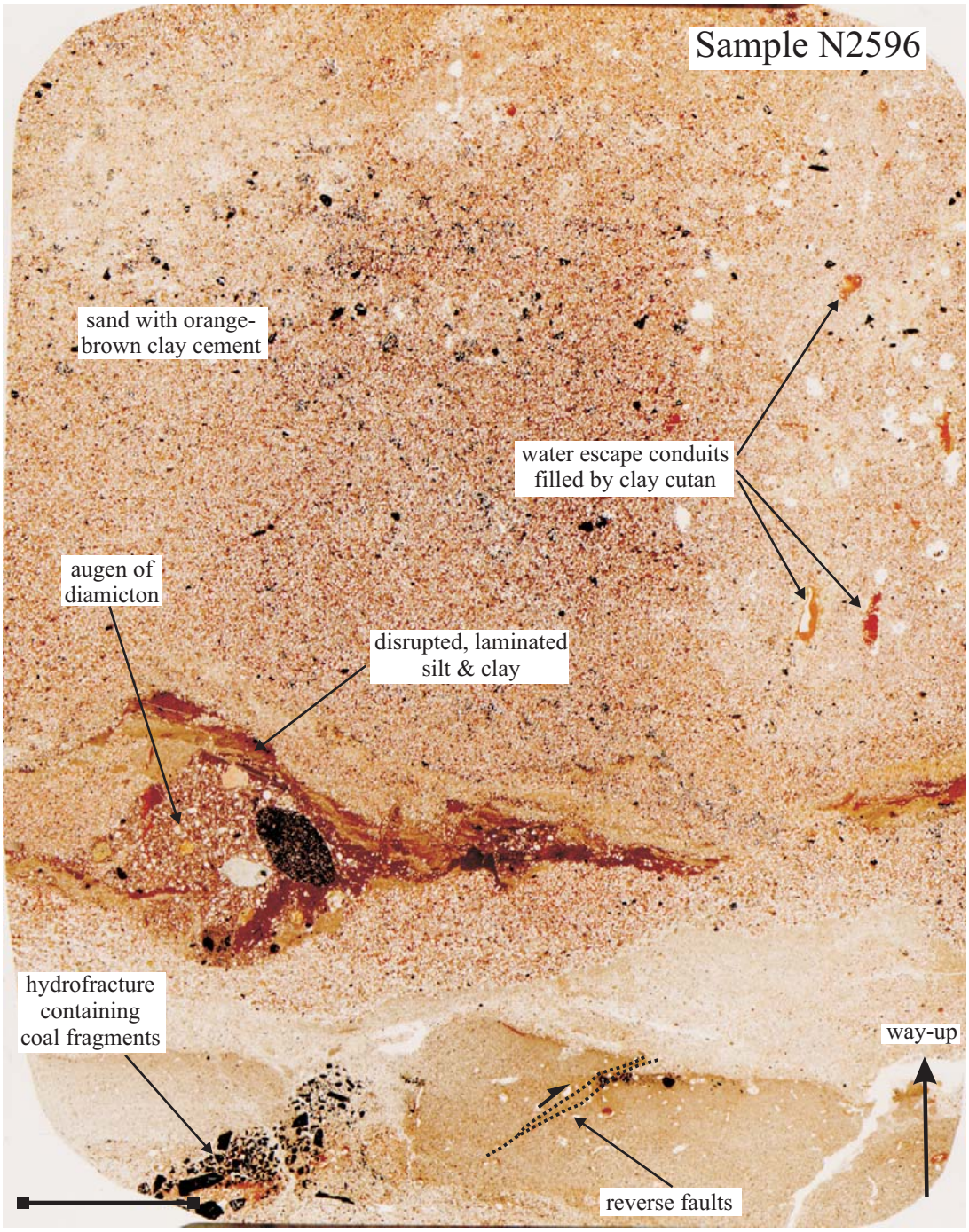

Figure 4. Annotated scanned image of the large format thin section taken from sample N2596 (see text for details). Scale bar = 10 mm.

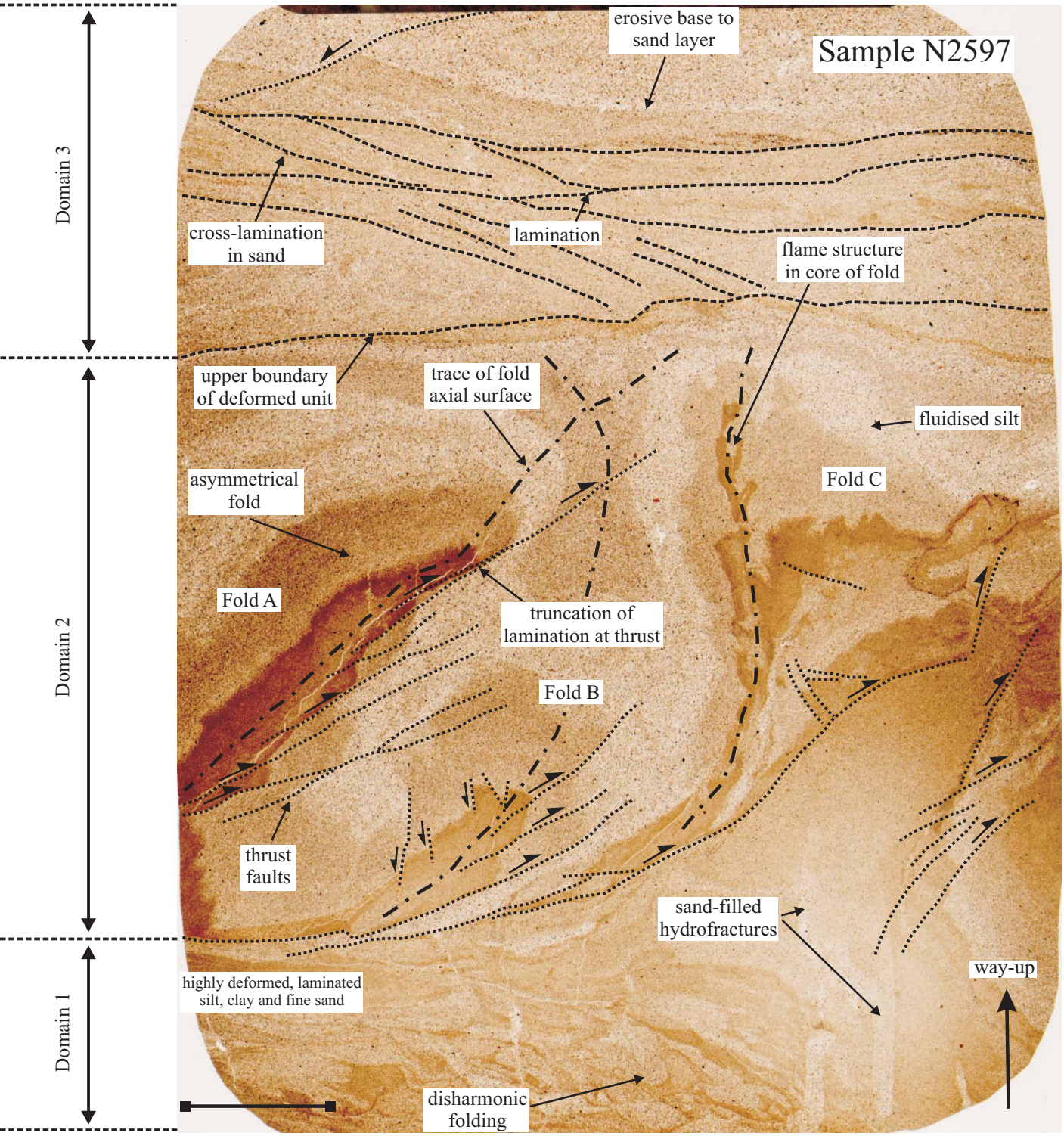

Figure 5. Annotated scanned image of the large format thin section taken from sample N2597 (see text for details). Scale bar = 10 mm.

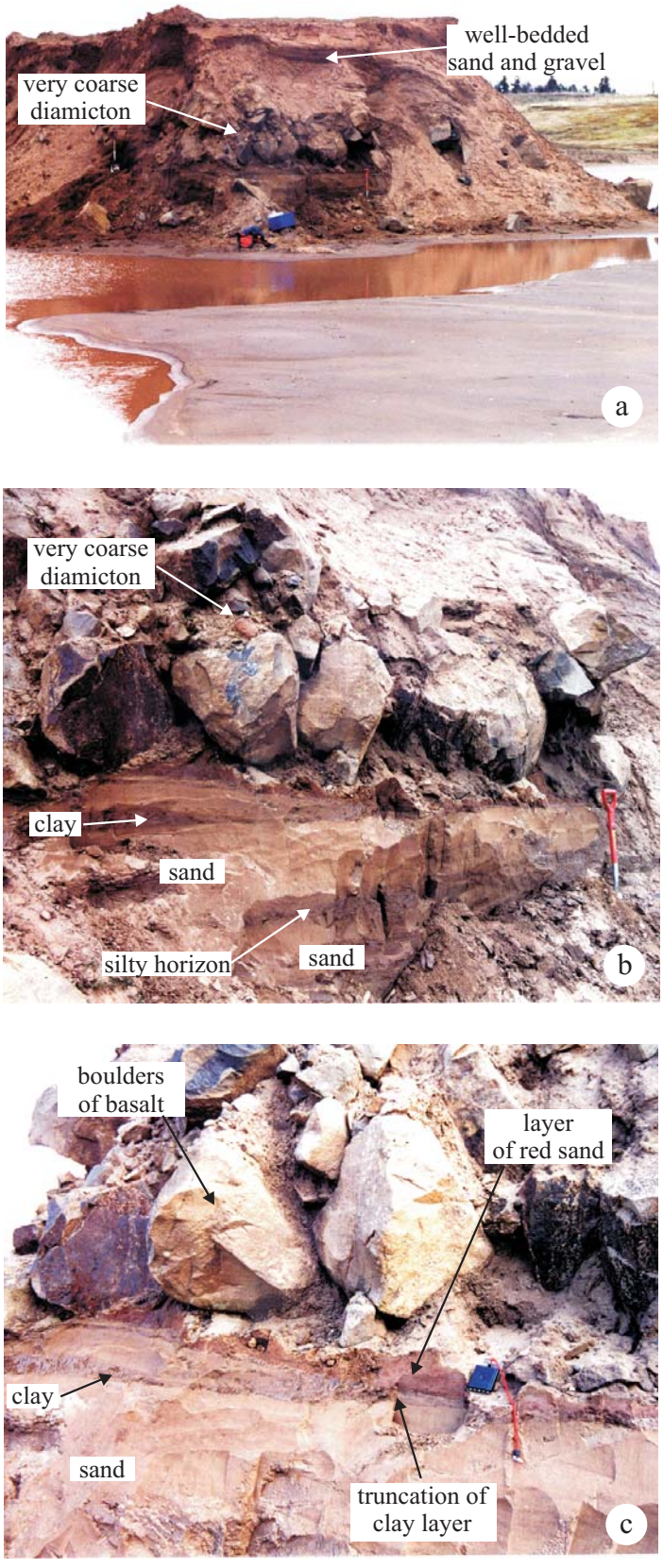

Plate 1. (a) General view of section exposed in Westend Wood sand and gravel quarry. The sand-dominated sequence also contains a very coarse diamicton with 1 to 1.5 m diameter boulders of basalt. **(b)** Lower boundary separating the diamicton and the underlying sand-dominated glaciofluvial sequence. Note that there is a distinctive clay and laminated silt-sand layer at the base of the diamicton, and that there is a lack of obvious disturbance within the underlying sediments. **(c)** Lower boundary of the diamicton showing truncation of the clay layer and presence of a red coloured sandy horizon at the contact between the diamicton and underlying sediments.

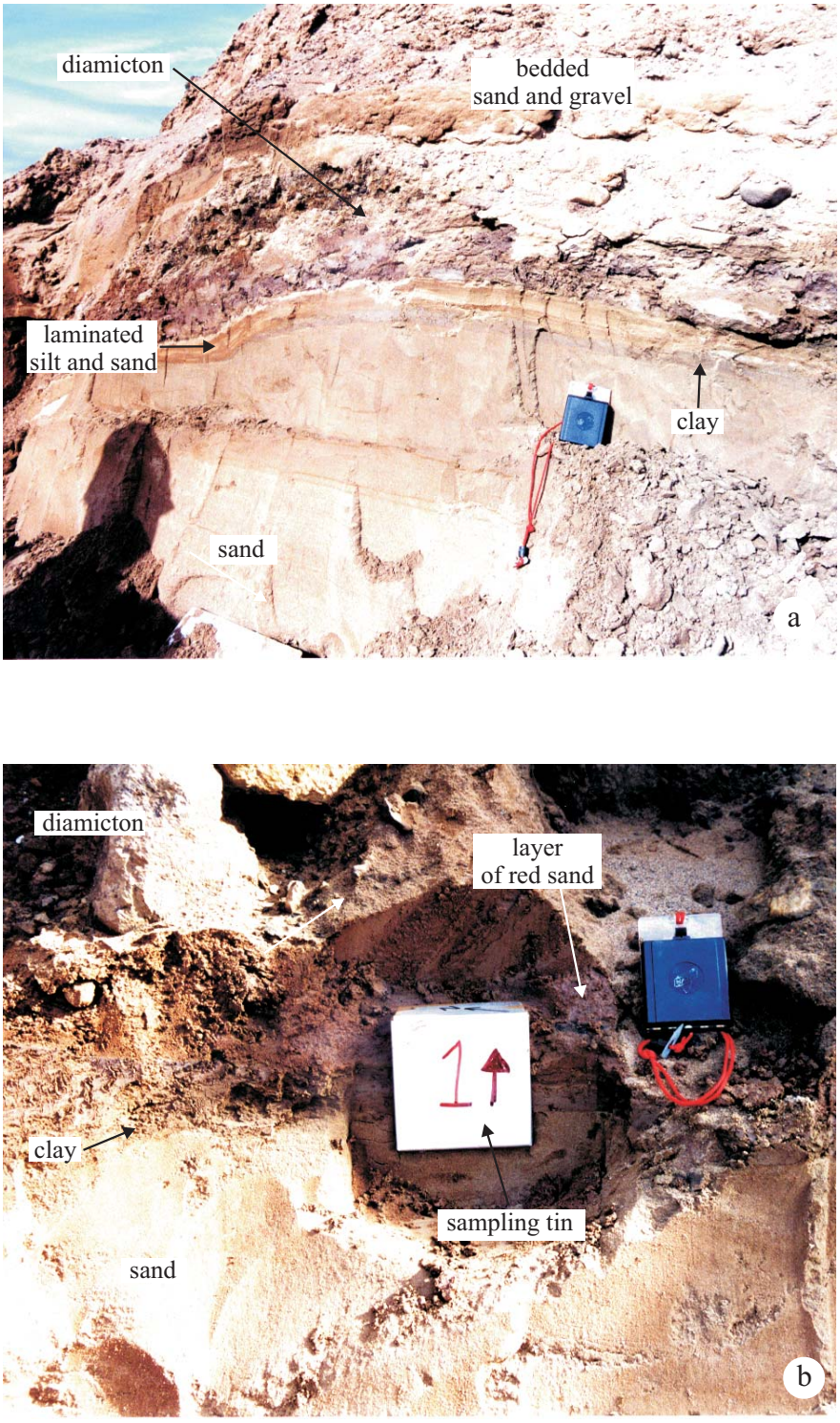

Plate 2. (a) Bedded sand and gravel sequence in which the diamicton lacks the large boulders of basalt observed in the northern part of the section. **(b)** Close-up of boundary between the very coarse diamicton and the underlying sand-dominated sediments. The boundary between the two units is marked by clay, overlain by laminated silt and sand, followed by red-coloured sand. A sample tin has been inserted into the face across this complex sequence.

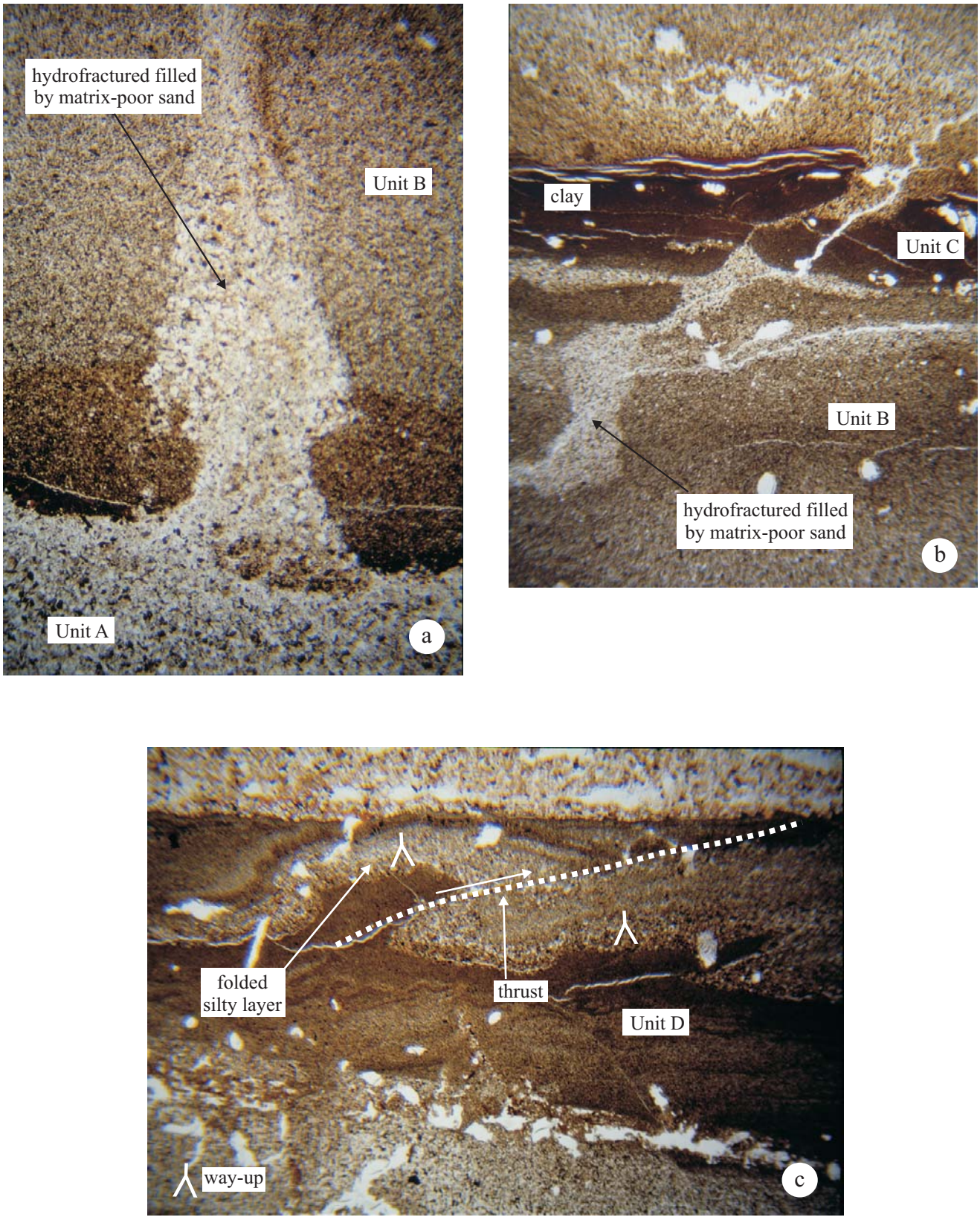

Plate 3. Photomicrographs of: **(a)** Hydrofracture filled by fine-grained, matrix-poor sand (scale bar = 2 mm); **(b)** Complex pattern of sand-filled hydrofractures with horizontal, bedding-parallel features occurring immediately below a prominent clay layer (see text for details) (scale bar = 2 mm); and **(c)** Small-scale folding and thrusting of a graded silt lamina (Scale bar = 2 mm). (sample N2593; plane polarised light).

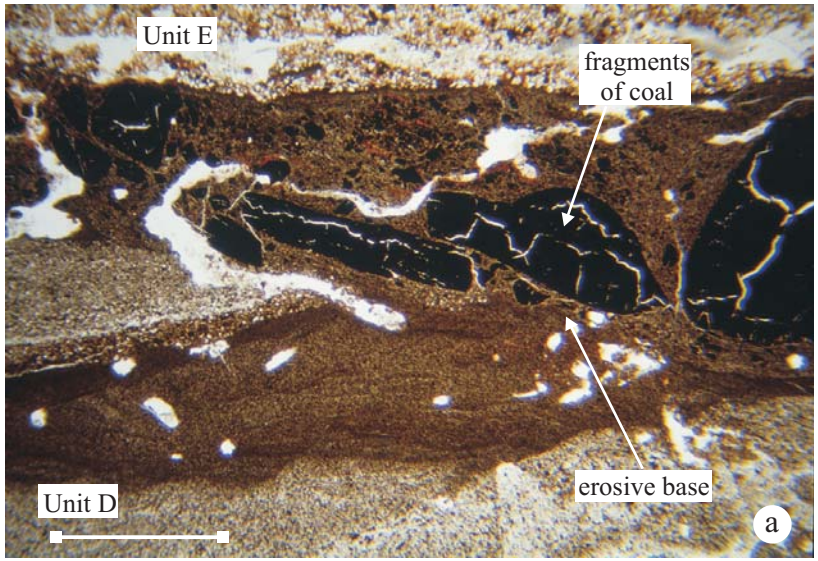

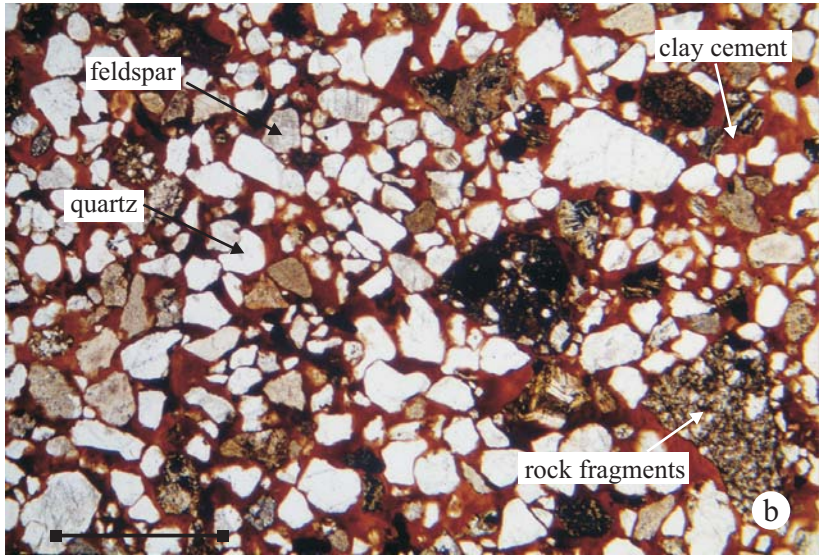

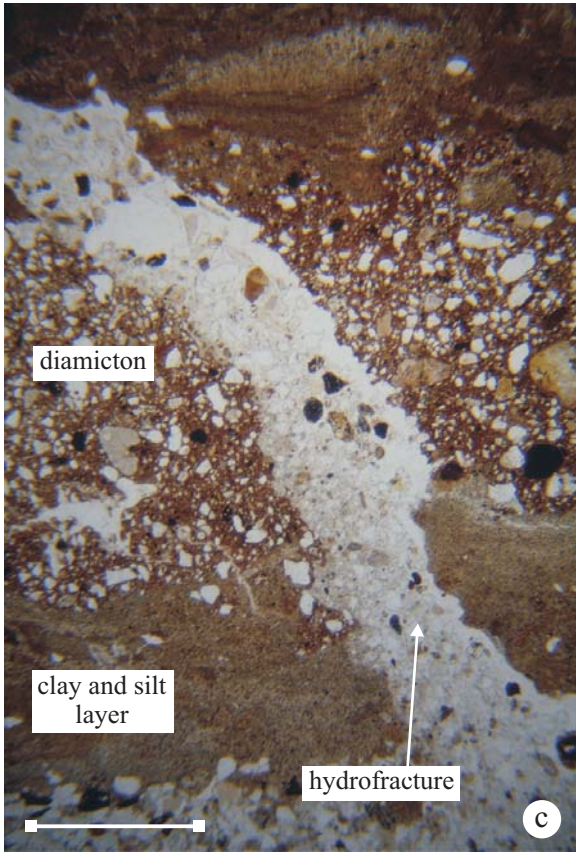

Plate 4. Photomicrographs of: **(a)** Lenticular silty lamina containing fragments of coal cross-cutting laminated silt and clay (scale bar = 2 mm); **(b)** Poorly sorted sand with an open packed, 'cement supported' texture. Cement composed of a distinctive orange-brown clay (scale bar = 1 mm); and **(c)** Hydrofracture filled by fine-grained sand to coarse silt cross-cutting stratification in basal part of the diamicton (Scale bar = 2 mm). (a and b - sample N2593, c - sample N2594; plane polarised light).

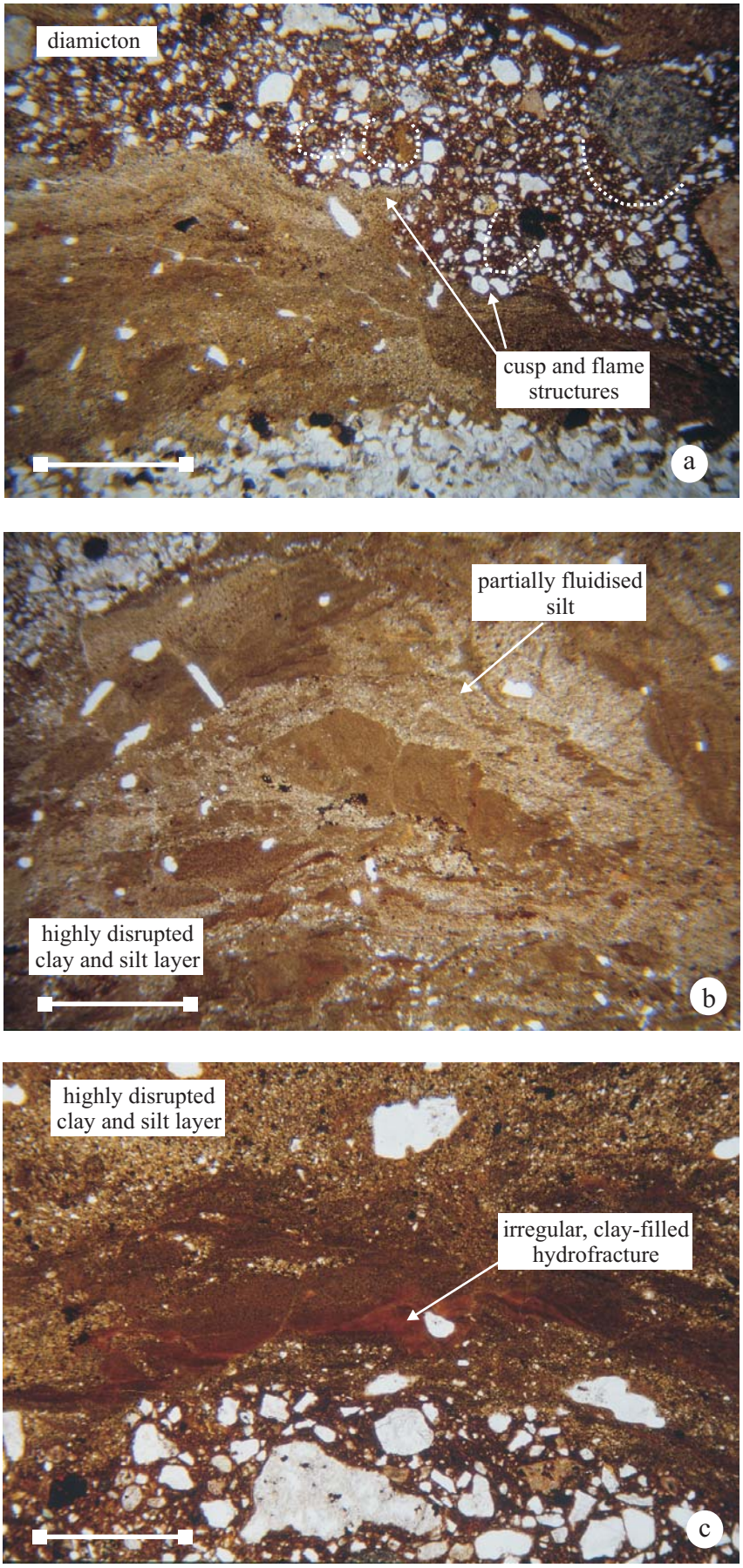

Plate 5. Photomicrographs of: **(a)** Stratification within basal part of diamicton. Note cusp and flame structures developed along the boundary between the silt and clay layer and the adjacent diamicton, as well as the presence of circular and arcuate grain alignment structures within the matrix of the diamicton (scale bar = 2 mm); **(b)** Highly disrupted silt and clay layer within the diamicton characterised by the fragmentation of the more clay-rich laminae and partial liquefaction of the associated silt (scale bar = 2 mm); and **(c)** Wispy looking hydrofracture within a highly disrupted silt and clay layer filled by an orange-brown clay cutan (Scale bar = 2 mm). (sample N2594; plane polarised light).

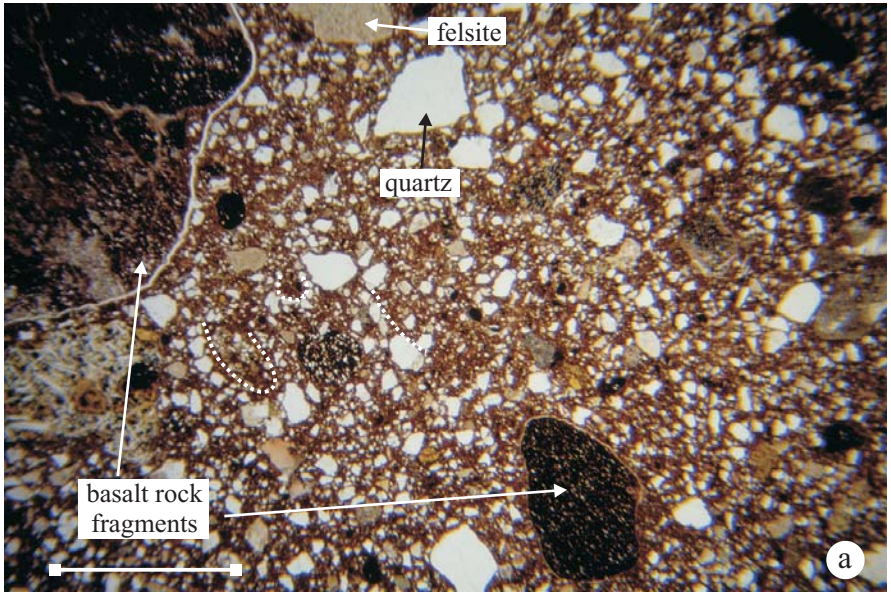

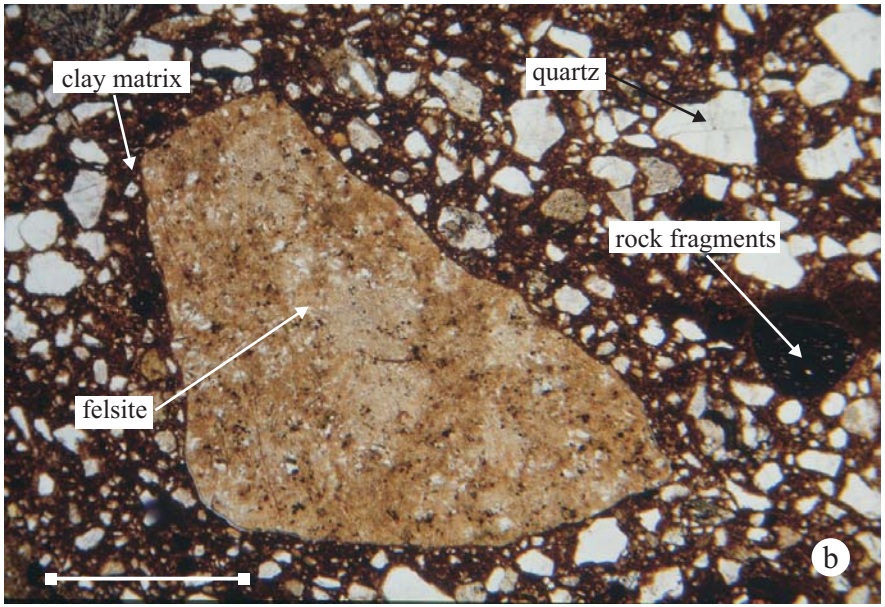

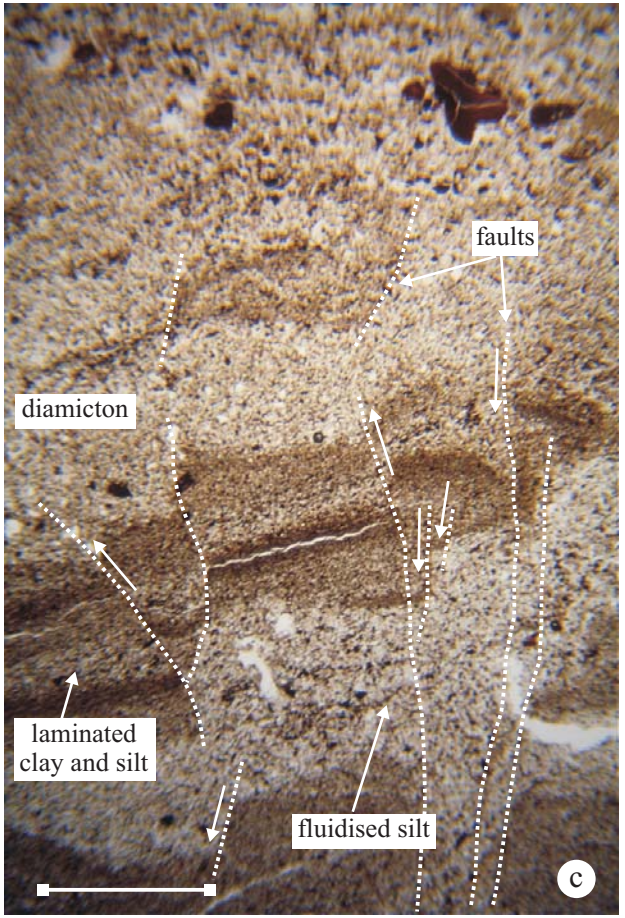

Plate 6. Photomicrographs of: **(a)** Poorly sorted, matrix supported diamicton containing subrounded clasts of basalt, as well as more angular quartz and felsite (rhyolite) fragments (scale bar = 2 mm); **(b)** Poorly sorted diamicton containing a large, angular to subangular felsite (rhyolite) rock fragment. Also note there is a slightly more clay-rich coating developed upon the lithic clast (scale bar = 2 mm); and **(c)** High-angle normal and reverse faults off-setting laminated clay and silt. Also note preferential fluidisation of the clay-poor, slightly coarser grained silt laminae (Scale bar = 2 mm). (a and b - sample N2594, c - sample N2595; plane polarised light).

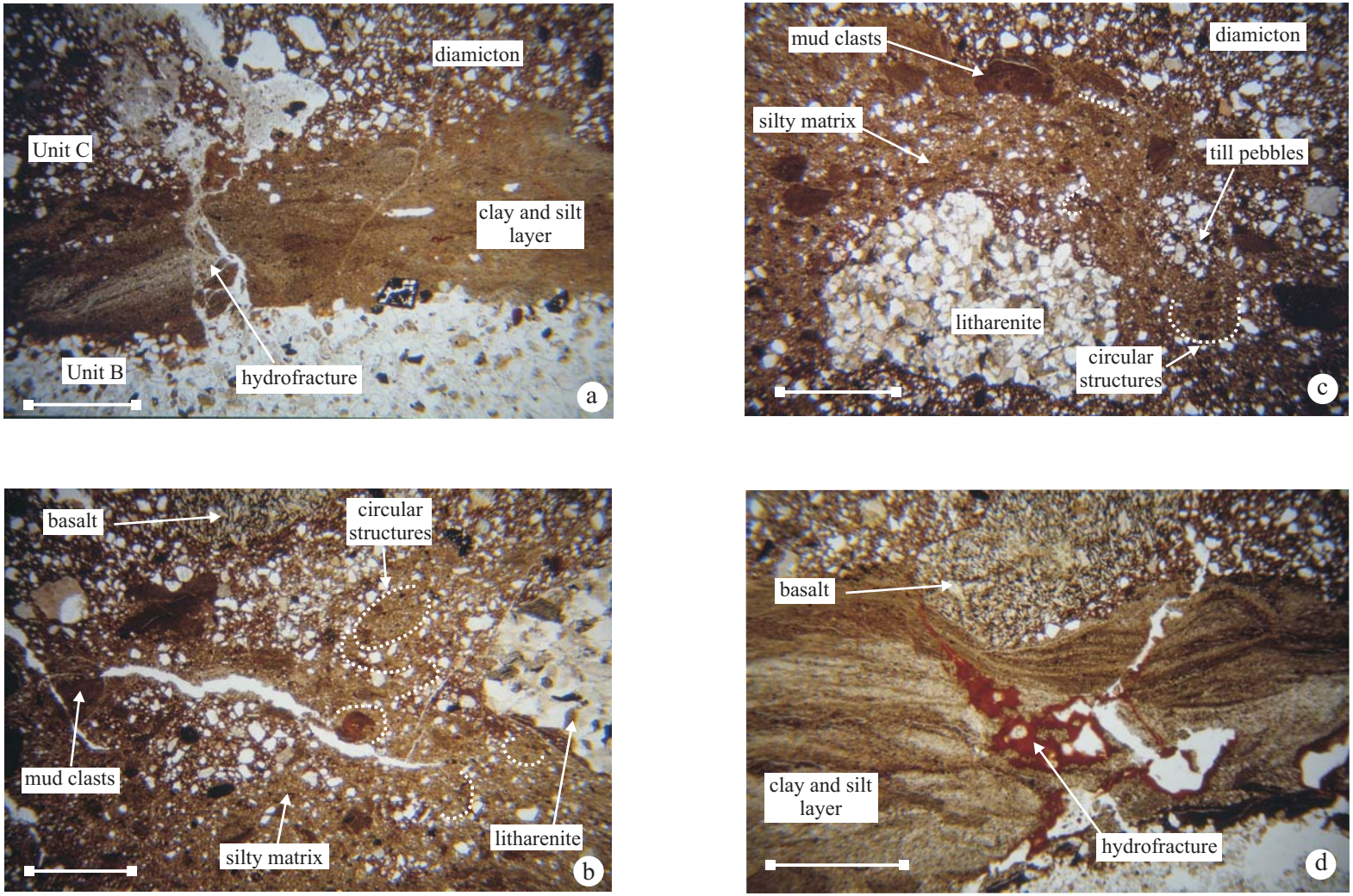

Plate 7. Photomicrographs of: **(a)** Boundary between stratified diamicton and underlying matrix-poor sand of Unit B. This boundary is deformed by a irregular silt-filled hydrofracture (scale bar = 2 mm); **(b)** Highly disrupted silty layer within the diamicton containing lithic fragments and till pebbles derived from the adjacent diamicton layers. Original clay laminae have been fragmented to form variably rounded mud clasts. Also note the presence of circular grain alignments within this silty layer (scale bar = 1 mm); **(c)** Highly disrupted silty layer within the diamicton (Unit C) containing lithic fragments and till pebbles derived from the adjacent diamicton layers. Original clay laminae have been fragmented to form variably rounded mud clasts (Scale bar = 2 mm); and **(d)** Finely laminated silt and clay layer at the base of the stratified diamicton (Unit C). The layer is cut by an irregular hydrofracture filled by an orange-brown clay cutan (scale bar = 2 mm). (sample N2595; plane polarised light).

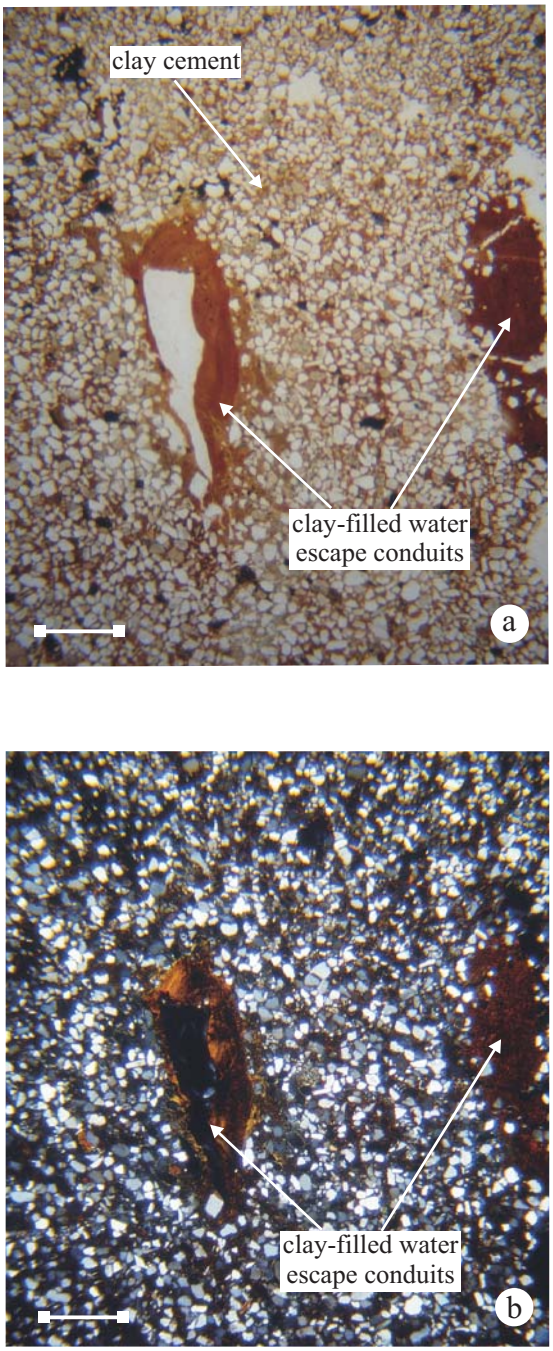

Plate 8. Photomicrograph of a moderately to poorly sorted, fine-grained sand with a variably developed clay cement. Also present are two elongate water escape conduits filled by an orange-brown, strongly birefringent clay cutan (scale bar = 2 mm). (sample N2596; a - plane polarised light, b - crossed polarised light).

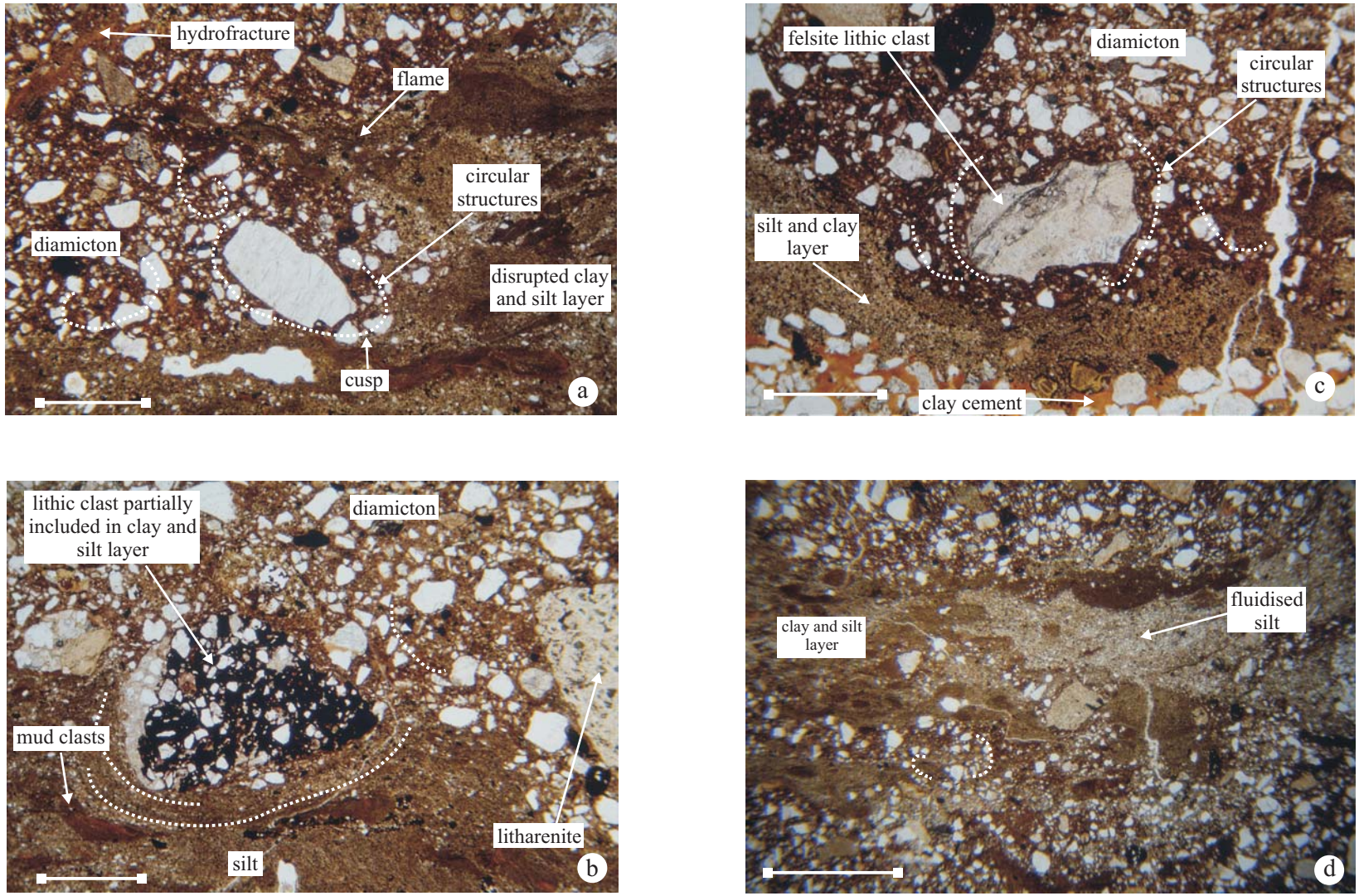

Plate 9. Photomicrographs of: **(a)** Cusp and flame structure deforming boundary of a disrupted silt and clay layer within the stratified diamicton. Also note the presence of a circular arrangement of detrital grains (galaxy structure) within the diamicton which corresponds to the cusp formed at the boundary with the adjacent silt and clay layer (scale bar = 1 mm); **(b)** Lithic clast partially included within a disrupted silty layer (scale bar = 1 mm); **(c)** Cusp structure deforming boundary of a disrupted silt and clay layer within the stratified diamicton. Also note the presence of a circular arrangement of detrital grains (galaxy structure) within the diamicton which corresponds to the cusp formed at the boundary with the adjacent silt and clay layer (Scale bar = 1 mm); and **(d)** Highly disrupted silt and clay layer in which the silt laminae have undergone liquefaction (scale bar = 2 mm). (sample N2594; plane polarised light).

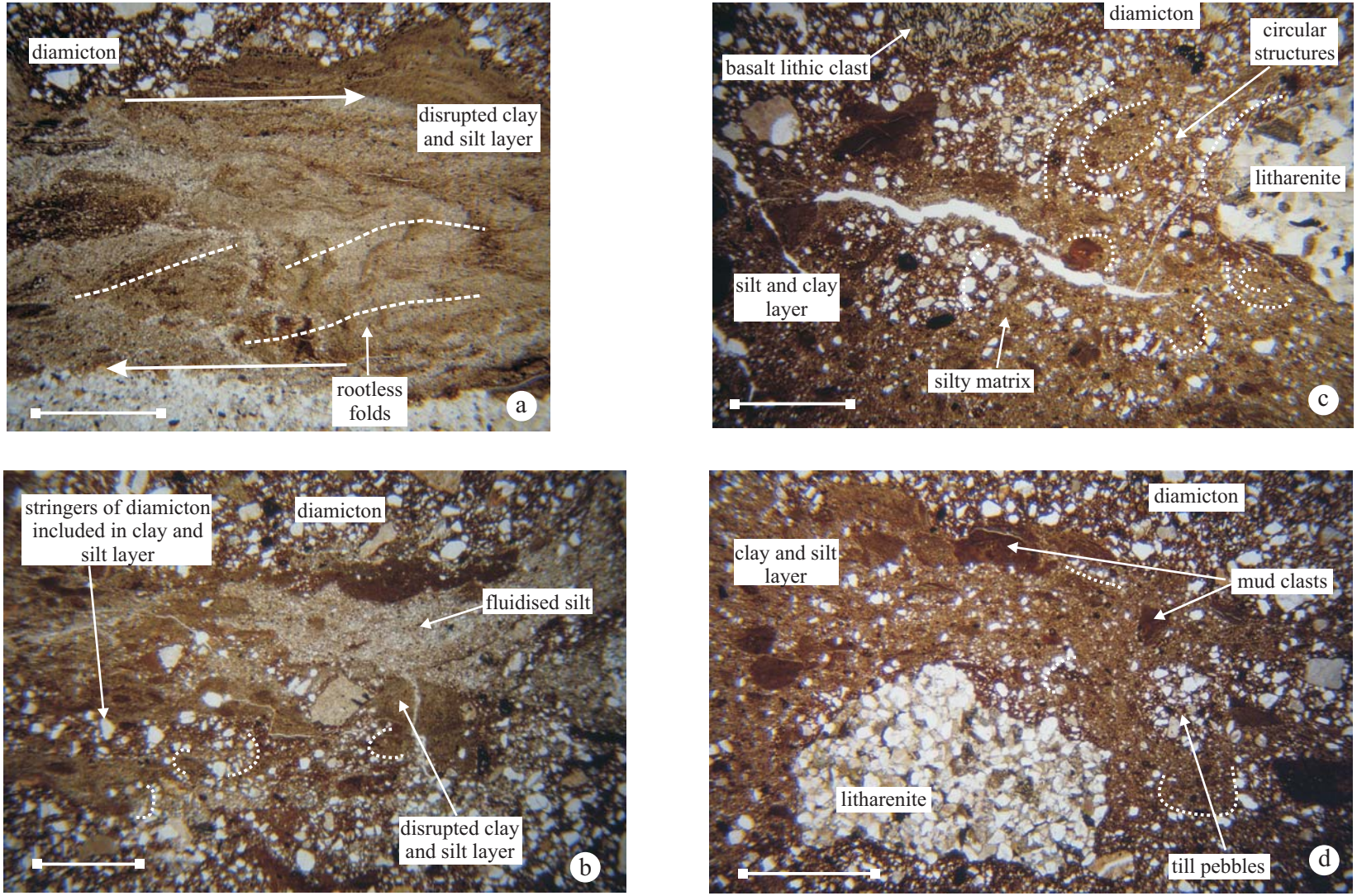

Plate 10. Photomicrographs of: **(a)** Folding within a disrupted silt and clay layer at the base of the stratified diamicton (scale bar = 2 mm); **(b)** Highly disrupted silt and clay layer containing stringers of diamicton. Also note that the silt laminae have undergone liquefaction (scale bar = 2 mm); **(c)** Highly disrupted silty layer containing lithic fragments and till pebbles derived from the adjacent diamicton layers. Original clay laminae have been fragmented to form variably rounded mud clasts. Also note presence of circular and arcuate arrangements of clasts within this disrupted silty layer (Scale bar = 2 mm); and **(d)** Highly disrupted silty layer containing lithic fragments, mud clasts and till pebbles derived from the adjacent diamicton layers. Also note presence of circular and arcuate arrangements of clasts within this disrupted silty layer (scale bar = 2 mm). (a and b sample N2594, c and d sample N2595; plane polarised light).

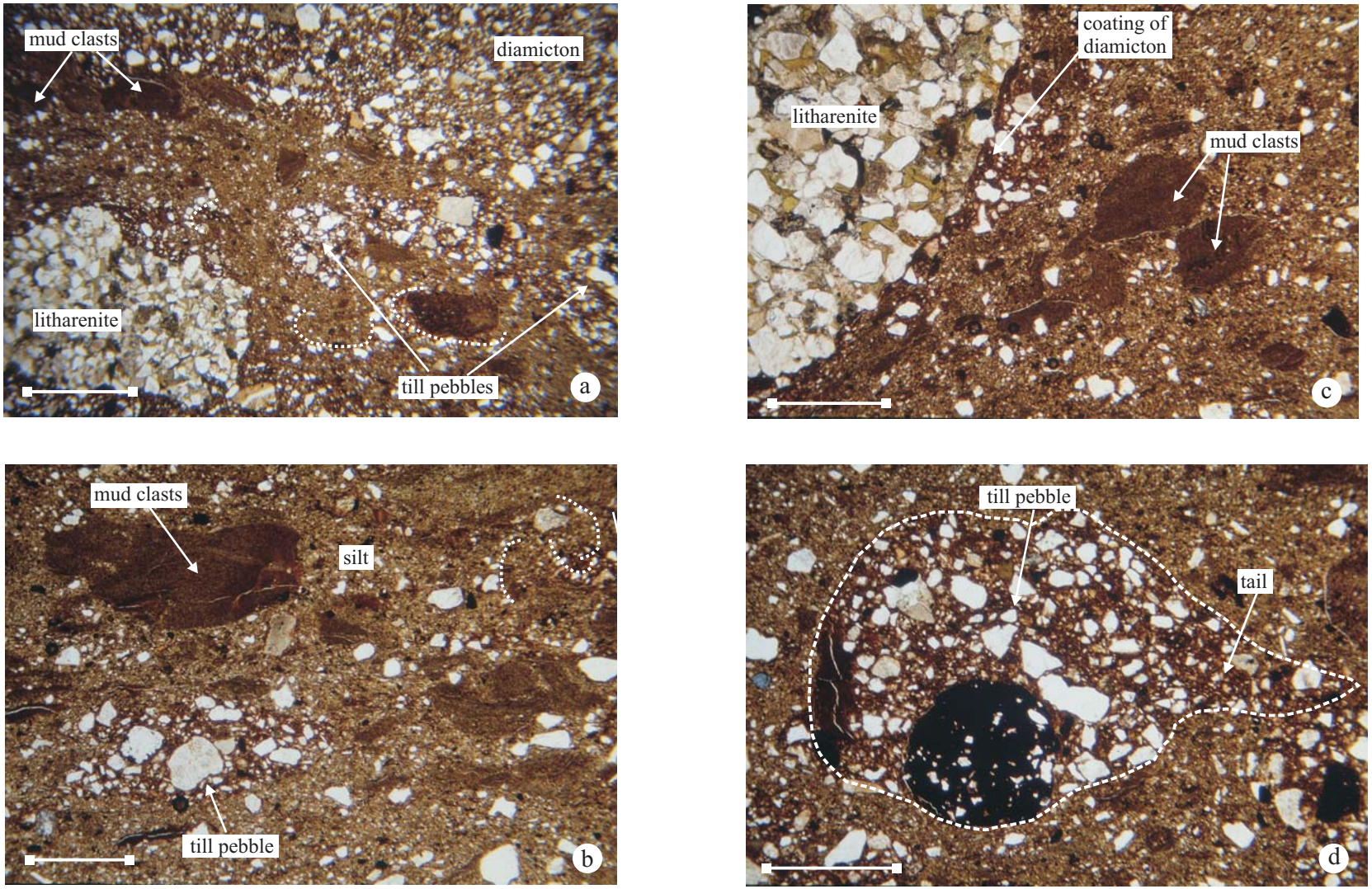

Plate 11. Photomicrographs of: **(a)** Folding within a disrupted silt and clay layer at the base of the stratified diamicton (scale bar = 2 mm); **(b)** Highly disrupted silt and clay layer containing stringers of diamicton. Also note that the silt laminae have undergone liquefaction (scale bar = 2 mm); **(c)** Highly disrupted silty layer containing lithic fragments and till pebbles derived from the adjacent diamicton layers. Original clay laminae have been fragmented to form variably rounded mud clasts. Also note presence of circular and arcuate arrangements of clasts within this disrupted silty layer (Scale bar = 2 mm); and **(d)** Highly disrupted silty layer containing lithic fragments, mud clasts and till pebbles derived from the adjacent diamicton layers. Also note presence of circular and arcuate arrangements of clasts within this disrupted silty layer (scale bar = 2 mm). (a and b sample N2594, c and d sample N2595; plane polarised light).